Research paper – *Global Ecology and Biogeography*

# Functional biogeography of Neotropical moist forests: trait-climate relationships and assembly patterns of tree communities

**Running title:** Functional biogeography of Neotropical forests

Bruno X. Pinho[1*], Marcelo Tabarelli[1], Cajo ter Braak[2], S. Joseph Wright[3], Víctor Arroyo-Rodríguez[4,5], Maíra Benchimol[6], Bettina M. J. Engelbrecht[7,3], Simon Pierce[8], Peter Hietz[9], Bráulio A. Santos[10], Carlos A. Peres[10,11], Sandra C. Müller[12], Ian J. Wright[13], Frans Bongers[14], Madelon Lohbeck[14,15], Ülo Niinemets[16], Martijn Slot[3], Steven Jansen[17], Davi Jamelli[1], Renato A.F. de Lima[18,19], Nathan Swenson[20], Richard Condit[21,22], Jos Barlow[23], Ferry Slik[24], Manuel A. Hernández-Ruedas[4], Gabriel Mendes[1], Miguel Martínez-Ramos[4], Nigel Pitman[25], Nathan Kraft[26], Nancy Garwood[27], Juan Ernesto Guevara Andino[28], Deborah Faria[6], Eduardo Chacón[29], Eduardo Mariano-Neto[30], Valdecir Júnior[10], Jens Kattge[31,32], and Felipe P.L. Melo[1]

[1]Departamento de Botânica, Universidade Federal de Pernambuco, Recife, Brazil

[2]Biometris, Wageningen University & Research, Wageningen, The Netherlands

[3]Smithsonian Tropical Research Institute, Balboa, Republic of Panama

[4]Instituto de Investigaciones en Ecosistemas y Sustentabilidad, Universidad Nacional Autónoma de México, Morelia, Mexico

[5]Escuela Nacional de Estudios Superiores, Universidad Nacional Autónoma de México, Mérida, Mexico

[6]Departamento de Ciências Biológicas, Universidade Estadual de Santa Cruz, Ilhéus, Brazil

[7]Department of Plant Ecology, Bayreuth Center of Ecology and Environmental Research, University of Bayreuth, Bayreuth, Germany

[8]Department of Agricultural and Environmental Sciences, University of Milan, Milan, Italy

[9]Institute of Botany, University of Natural Resources and Life Sciences, Vienna, Austria

[10]Departamento de Sistemática e Ecologia, Universidade Federal da Paraíba, João Pessoa, Brazil

[11]School of Environmental Sciences, University of East Anglia, Norwich Research Park, Norwich, UK

[12]Departamento de Ecologia, Universidade Federal do Rio Grande do Sul, Porto Alegre, Brazil

[13]Department of Biological Sciences, Macquarie University, Sydney, Australia

[14]Forest Ecology and Forest Management group, Wageningen University & Research, Wageningen, The Netherlands

[15]World Agroforestry (ICRAF), Nairobi, Kenya

[16]Estonian University of Life Sciences, Tartu, Estonia

[17]Institute of Systematic Botany and Ecology, Ulm University, Ulm, Germany

[18]Departamento de Ecologia, Universidade de São Paulo, São Paulo, Brasil

[19]Tropical Botany, Naturalis Biodiversity Center, Leiden, The Netherlands

[20]Department of Biology, University of Maryland, Maryland, U.S.A.

[21]Field Museum of Natural History, Chicago, USA

[22]Morton Arboretum, Illinois, USA

[23]Lancaster Environment Centre, Lancaster University, United Kingdom

[24]Faculty of Science, Universiti Brunei Darusallam, Gadong, Brunei

[25]Department of Botany, Duke University, North Carolina, U.S.A.

[26]Department of Ecology and Evolutionary Biology, University of California, Los Angeles, U.S.A.

[27]School of Biological Sciences, Southern Illinois University, Carbondale, U.S.A.

[28]Grupo de Investigación en Biodiversidad Medio Ambiente y Salud, Universidad de las Américas, Quito, Ecuador.

[29]Escuela de Biología, Universidad de Costa Rica, San José, Costa Rica

[30]Instituto de Biologia, Universidade Federal da Bahia, Salvador, Brazil

[31]Max Planck Institute for Biogeochemistry, Jena, Germany

[32]German Centre for Integrative Biodiversity Research, Halle-Jena-Leipzig, Germany

*Corresponding author: bxpinho@hotmail.com

**Abstract**

**Aim**: Here we examine the functional profile of regional tree species pools across the latitudinal distribution of Neotropical moist forests, and test trait-climate relationships among local communities. We expected opportunistic strategies (acquisitive traits, small seeds) to be overrepresented in species pools further from the equator, but also in terms of abundance in local communities in currently wetter, warmer and more seasonal climates.

**Location**: Neotropics.

**Time period**: Recent.

**Major taxa studied**: Trees.

**Methods**: We obtained abundance data from 471 plots across nine Neotropical regions, including ~100,000 trees of 3,417 species, in addition to six functional traits. We compared

occurrence-based trait distributions among regional species pools, and evaluated single trait-climate relationships across local communities using community abundance-weighted means (CWM). Multivariate trait-climate relationships were assessed by a double-constrained correspondence analysis that tests both how CWMs relate to climate and how species distributions, parameterized by niche centroids in climate space, relate to their traits.

**Results**: Regional species pools were undistinguished in functional terms, but opportunistic strategies dominated local communities further from the equator, particularly in the northern hemisphere. Climate explained up to 57% of the variation in CWM traits, with increasing prevalence of lower-statured, light-wooded and softer-leaved species bearing smaller seeds in more seasonal, wetter and warmer climates. Species distributions were significantly but weakly related to functional traits.

**Main conclusions**: Neotropical moist forest regions share similar sets of functional strategies, from which local assembly processes, driven by current climatic conditions, select for species with different functional strategies. We can thus expect functional responses to climate change driven by changes in relative abundances of species already present regionally. Particularly, equatorial forests holding the most conservative traits and large seeds are likely to experience the most severe changes if climate change triggers the proliferation of opportunistic tree species.

*Key-words*: climate change, climate seasonality, community assembly, functional composition, functional traits, latitude, precipitation, species pool, temperature.

## Introduction

Plants have evolved a broad range of functional strategies to cope with diverse environmental conditions (Díaz et al., 2016; Pierce et al., 2017). The functional assembly of plant communities results from the interplay among eco-evolutionary forces operating at different spatial-temporal scales (Kraft & Ackerly, 2014). At regional scales, the diverse functional strategies found in any given species pool reflect long-term speciation, dispersal and extinction filters (Mittelbach & Schemske, 2015). For instance, long-term climatic instability and natural disturbance regimes, such as hurricanes, storms and forest expansion-retraction dynamics due to glacial cycles, may select for functional profiles that favor population persistence under unstable conditions, while disturbance-sensitive species may be rare of even absent from regions under such conditions (Balmford, 1996; Betts et al., 2019). At local scales, the functional profile of plant communities depends on the filtering of regionally available species across varying current climate regimes (Swenson et al., 2012; Cadotte & Tucker, 2017). Assessing changes in functional composition of regional species pools and local communities along wide (bio)geographic and climatic gradients can help to understand potential responses to climate change and other human-caused disturbances (Violle et al., 2014). For instance, global climate change will soon bring unprecedented extreme climates to the Neotropics (Mora et al., 2013). Therefore, assessing how tree communities are functionally structured by trait-climate relationships helps predict the future of Neotropical forests in a rapidly changing world.

The advent of global plant trait databases in recent decades has enabled numerous investigations of patterns of trait variation and their relationships with climatic and biogeographic gradients (e.g., Swenson et al., 2012). These studies have revealed intriguing patterns, such as the tendency of plant species in warmer and less seasonal sites (closer to the

equator) to be taller and bear larger and softer leaves, larger seeds and denser woods (Wright et al., 2004, 2017; Moles et al., 2007, 2009; Swenson et al., 2012). However, these large-scale trait patterns were described mostly from species occurrence data across spatial grid-cells or latitudinal bands, and therefore failed to account for ecological processes operating at local scales that govern abundance of species and ultimately the functional profile of plant assemblages. On the other hand, studies that have assessed variation in abundance of species and their traits in local communities are based on either a single regional flora (e.g., van der Sande et al., 2016) or a single trait (e.g., Swenson & Enquist, 2007), and thus are unable to capture species assembly processes along wide biogeographic and climatic gradients. Scaling up abundance-based analyses of local communities to biogeographic scales can improve our understanding about climatic effects on local trait dominance, which ultimately drives ecosystem functioning (Poorter et al., 2017). In this way, Bruelheide et al. (2018) recently used a large dataset to examine global trait-environment relationships at the local community level (including abundance data), and found only weak support ($R^2 < 0.1$) for trait-climate relationships. These global-scale analyses, though insightful, can mask relevant patterns within biotas that share a relatively common (but diverse) biogeographic history, such as Neotropical moist forests.

Neotropical moist forests extend from southern Mexico to northern Argentina and represent an enormous variation in past and current climatic conditions (Frierson et al., 2013; Blonder et al., 2018) and biogeographic histories (Gentry, 1982; Burnham & Graham, 1999). Overall, these differences clearly result in distinct taxonomic and phylogenetic composition more or less packed into biogeographic provinces. For instance, tropical moist forests of Meso-America (including Mexico) are taxonomically distinct from those in South America; the flora of the latter being mostly of Gondwanan origin while the northern Neotropics supports many plant

lineages with Laurasian affinity (Gentry, 1982; Graham, 1999). Also, palynological evidence points to a higher frequency of past disturbance events and faster recovery of tropical forests in northern Central America compared to South American counterparts (Cole et al., 2014). Mexican forests are the northern limit of the Neotropical forest distribution and experienced repeated expansion-retraction cycles due to Pleistocene glaciations (Burnham & Graham, 1999; Graham, 1999), compared to South America, where many large blocks of forests remained stable during the last glacial and the influence of the Andes and the South American dry diagonal corridor is remarkable (Colinvaux et al., 2000; Hoorn et al., 2010; Leite et al., 2016).

While assessing relationships between traits and current climate is straightforward, addressing the effects of biogeographic history is challenging. Historical contingencies such as speciation/extinction dynamics and dispersal events must have affected the functional structure of current species pools and different drivers might act across localities (Fukami, 2015). Distance from the equator is related to current climate seasonality but has also been used as a proxy of biogeographic history, from plants to mammals, given its correlation to past cycles of climate change (Dynesius & Jansson, 2000; Betts et al., 2019). It is thus reasonable to expect that tropical biotas far from the equator experienced, currently and in the past, more shifting climates than their equatorial counterparts (Blonder et al., 2018; Betts et al., 2019). Such instability might select for opportunistic strategies related to fast growth and high dispersal ability. For instance, northern forests are mostly composed of broad-ranged plant species due to short- and long-term climatic instability, while small-ranged species concentrate under stable climates in Central America, Amazonia and Atlantic forests (Morueta-Holme et al., 2013), which are relatively equatorial regions that also support higher phylogenetic endemism (Sandel et al., 2020). In contrast, extreme southern Neotropical vegetation has developed under relatively low and

157 seasonal temperature and precipitation levels (Oliveira-Filho et al., 2013). The extent to which
158 such historical contingencies can induce distinct signatures on the functional composition of
159 Neotropical moist forests is yet to be fully understood.

160 Several key aspects of community functional composition can be expressed through the
161 'global spectrum of plant form and function' (Díaz et al., 2016). Specifically, plants well adapted
162 to resource-poor/stressful environments with low disturbance regimes tend to grow slowly (i.e.,
163 low metabolic resource demand) and invest in dense, durable tissues (i.e., conservative traits). In
164 contrast, acquisitive resource-use traits (e.g., low-density woods, soft leaves) favor hydraulic
165 efficiency and rapid plant growth, allowing resource pre-emption in productive habitats such as
166 those under wetter and warmer climates (Westoby et al., 2002; Reich, 2014). Such opportunistic
167 strategy can also benefit under more seasonal climates by optimizing carbon gain during the
168 growing season in the more open forests that allow more light to reach the understory (Kobe,
169 1999; Kikuzawa et al., 2013). Regarding size-related traits, increasing leaf area favors light
170 capture, but limits heat exchange with the surrounding air, and leads to a higher daytime
171 transpirational water loss, thereby being favored in warm, moist and sunny environments
172 (Wright et al., 2017). Also, larger seeds may promote higher seedling performance under low
173 resource availability (Leishman & Westoby, 1994; Muller-Landau, 2010), while smaller-seeded
174 species have greater seed output that favors dispersal to recently disturbed sites and seeds that
175 are more likely to exhibit dormancy, which favors survival under variable climates (de Casas et
176 al., 2017). Finally, larger trees tend to have greater access to light and belowground resources,
177 but are more prone to hydraulic failure during drought (Brum et al., 2019). Combinations of
178 these traits define ecological strategies that influence plant responses to environmental
179 conditions (Grime & Pierce, 2012).

Here we test two mutually compatible effects of biogeographic history and current climate as structuring drivers of the functional organization of tree communities across Neotropical moist forests. If historical contingency prevails, then we should expect functional dissimilarities among regional tree species pools, which could lead to differences in functional composition of local communities occurring in similar climates at different regions. If current climate represents a prevailing force, functional differences should emerge at the local scale due to changes in trait dominance in response to climatic conditions. In particular, we expected that regional species pools should be composed of different sets of functional strategies, with higher prevalence of species with opportunistic ecological strategies (i.e., low-density tissues, small seeds) in regions further from the equator due to long-term instability that selects for fast-growth and high dispersal ability. Across local communities, more seasonal, wetter and warmer climates should favor dominance of opportunistic strategies. We additionally assessed the consistency of trait-climate relationships by evaluating to what extent the distribution of species, expressed as the abundance-weighted mean climatic conditions at which they are found (i.e., niche centroids), is mediated by functional traits. We discuss our results in terms of how useful they are for the understanding of both community assembly patterns and potential responses of Neotropical tree floras to climate change and anthropogenic disturbances in human-dominated landscapes.

## Methods

*Study regions and plots*

We studied 471 forest plots from nine biogeographic regions distributed across the Neotropics, covering the whole latitudinal distribution of Neotropical moist forests (Fig. 1; see Table S1 in Supporting Information for details on sampling across regions). All plots were located in lowland

(up to 800 m a.s.l.), old-growth forests within a variable matrix of land uses. Mean annual precipitation ranged from 1,154 to 7,068 mm, and mean annual temperature from *c*. 17 to 28 ºC (Fig. S1). Temperature seasonality increases with distance from equator (Wright et al., 2009), while average temperature and precipitation are typically higher towards the northern Neotropics due to northward heat transport by ocean circulation (Frierson et al., 2013; Fig. 1).

*Vegetation data*

We used data from 96,290 live adult trees (stems with diameter at breast height, DBH ≥ 10 cm; excluding lianas and palms) belonging to 3,417 species. Tree inventories were carried out by the authors as described elsewhere (Pitman et al., 2001; Santos et al., 2008; Arroyo-Rodríguez et al., 2009; Faria et al., 2009; Hernández-Ruedas et al., 2014; Benchimol & Peres, 2015; Orihuela et al., 2015; Pinho et al., 2018) or compiled from the "Salvias" database through the Botanical Information and Ecology Network - 'BIEN' R package (Maitner et al., 2017), which includes the Gentry plots (Gentry, 1988). The sampled area and total number of individuals and species sampled by region are summarized in Table S1. The slight difference in sampling methods (e.g., plot sizes) should not affect our results as we focus on the *relative* dominance of functional traits and strategies within communities and the resulting variation across the Neotropics.

*Functional traits*

A comprehensive set of six traits was measured in the field (following Pérez-Harguindeguy et al., 2013) and compiled from global databases, such as 'TRY' (Kattge et al., 2020) and the 'Seed Information Database' – SID (Royal Botanic Gardens Kew, 2020). These traits are leaf area - LA [$cm^2$], specific leaf area – SLA [$cm^2/g$], leaf dry matter content –LDMC [mg/g], wood density –

WD [g/cm³], seed mass – SM [mg] and maximum height – Hmax [m]. We chose these traits because they are known to influence tree performance along climatic gradients (Westoby et al., 2002; Reich et al., 2014), and position species along the plant (and organ) economics and size-related traits spectra (Díaz et al., 2016; Pierce et al., 2017). For instance, the leaf and stem traits considered are expected to reflect a trade-off between rapid resource acquisition that enables growth in resource-rich environments (indicated by high SLA, low LDMC, low WD), and conservation of resources in well-protected tissues that ensure survival under low resource availability, indicated by the opposite traits (Reich, 2014).

For leaf traits in compound-leaved species, we considered leaflets as the sample unit. Although we recognize the importance of intraspecific trait variation in community assembly (Siefert et al., 2015), we used species' mean functional traits as we consider a meaningful approach for the purpose of this study due to the extensive species-level trait data and high species turnover among regions. Species-level trait data covered on average from 57 to 80% of total plot abundances across traits/regions (see Table S2 for a summary of trait coverage by region). For species with doubtful identification and/or no trait information, we first used average trait values at the genus level, then we imputed remaining missing values (for which no genus-level data were available) through multivariate trait imputation with chained equations by predictive mean matching, using the R package 'mice' (van Buuren & Groothuis-Oudshoorn, 2011). The imputed trait data represented 3% or less of individuals in plots for 40 of the 54 region-trait combinations and over 10% for just one combination (see Table S2 for a summary by region), and the distribution of the original and imputed datasets largely overlapped (Fig. S2). Genus-level trait means were well correlated with species mean traits (Table S3), and their inclusion led to similar distributions of CWM trait values (Fig. S3). These findings demonstrate

249 that our results are not due to spurious artefacts in the imputation of missing trait data. Also, the
250 exclusion of trees with DBH < 10 cm should not represent a significant bias because adults
251 covered the whole range of functional strategies evident among saplings, and abundance-
252 weighted distributions of species trait values largely overlap when considering smaller trees (see
253 example for Northern Meso-America, Fig. S4).
254
255 *Climate data*
256 For each plot, we assessed the average of five key bioclimatic variables that are thought to drive
257 trait distributions and vegetation patterns (Swenson et al., 2012; Moles, 2018). The five climatic
258 variables include mean annual precipitation (MAP), mean annual temperature (MAT),
259 precipitation seasonality (PS – coefficient of variation of monthly values), temperature
260 seasonality (TS – standard deviation of monthly values, multiplied by 100) and potential
261 evapotranspiration (PET – the amount of water expected to be removed by the atmosphere
262 through evapotranspiration processes annually). The first variables were obtained from
263 WorldClim version 2.0 (Fick & Hijmans, 2017), which is a high-resolution global geo-database
264 (30 arc seconds or ~ 1 km at equator) of monthly average data from 1970 to 2000. The PET was
265 calculated from a set of WorldClim variables (taken in the same timeframe as above), using an
266 equation proposed by the Food and Agriculture Organization of the United Nations, which
267 involves minimum, maximum and average temperature, solar radiation, wind speed and water
268 vapor pressure (Trabucco & Zomer, 2018). Other climatic variables were considered but then
269 excluded due to collinearity (see below, Table S4). The five climatic variables considered were
270 weakly inter-correlated (Table S4), but were strongly related to latitude (i.e., south-north
271 gradient) or degrees from equator (Fig. S1). Despite complex climate variability due to, for

example, ocean circulation and elevation (Frierson et al., 2013), in this dataset temperature seasonality was strongly positively correlated with degrees from equator, while other climatic variables (MAP, MAT, PET, PS) increased linearly from south to north (Fig. S1, see Fig. 1 for the overall climatic pattern across the Neotropics).

*Data analyses*

We log-transformed LA, SLA and SM values, and sqrt-transformed Hmax to reduce skewness in trait distributions. We also log-transformed MAP to reduce the influence of two exceptionally wet sites. Functional composition of regional species pools was described from distributions of the traits of species occurring in each region. Functional traits were scaled-up from the species-level to the plot-level by calculating the Community-Weighted Mean ('CWM' – i.e., species' trait values weighted by their relative abundances), which reflects the dominance of trait values in a community (Muscarella et al., 2017). CWM trait values were calculated using function 'functcomp' from the 'FD' R package (Laliberté & Legendre, 2010). To examine trait co-variation patterns among species and communities, we applied Principal Component Analyses to the species and CWM trait matrices, using the 'prcomp' R function (Venables & Ripley, 2002). We also computed CWM of species scores on the first two principal component axes, which should reflect economics and size trade-offs in functional strategies (Díaz et al., 2016).

To assess changes in community functional composition in response to climate or geography, we constructed separate linear mixed-effects models, for the CWM of each functional trait or strategy (i.e., species scores on the PCA axes, see above). The fixed effects were either the five bioclimatic variables described above or the geographic variables, latitude (to describe south-to-north gradients) and degrees from equator (to describe gradients toward

295 higher latitudes in both hemispheres). The random effect 'biogeographic region' was included in
296 all models to account for the nested structure of our sampling design, and to assess among-region
297 variation not explained by latitude or climate. To avoid multicollinearity between climatic or
298 geographic variables, we checked the variance inflation factor of each predictor in each model,
299 using the 'car' package for R. All values were < 3, which allowed us to include all five climate
300 variables or the two geographic variables in the models (Neter et al., 1996). After running a full
301 model with each set of predictors (i.e., climatic and geographic variables) for each response
302 variable (i.e., CWM of each trait and PCA axes scores) using the maximum likelihood method
303 with the R package 'lme4' (Bates et al., 2015), we tested all possible combinations of predictors
304 and performed a model selection procedure to select the best-fit models as those with lowest
305 Akaike Information Criterion values ($\Delta$AICc < 2). Then, we applied model averaging to make
306 inferences on how individual climatic variables influence CWM of traits and strategies, using the
307 'MuMin' R package (Barton, 2014).
308 To assess the variance in CWM of traits and strategies (i.e., species scores on principal
309 component axes, see above) among regions and the strength of their relationships with latitude or
310 climate, we partitioned the $R^2$ of each selected model into the total variance between-regions
311 ("conditional $R^2$") and the component explained by climate or latitude ("marginal $R^2$";
312 Nakagawa & Schielzeth, 2013), reporting the variance explained by the model with highest
313 marginal $R^2$ for each response variable. The difference between conditional and marginal $R^2$
314 values represents the variance between-regions not explained by climate/latitude (expressed as
315 fraction of the total variance). The within-region component is the remaining unexplained
316 variance (i.e., 1 – conditional $R^2$). For this, we used the R package 'piecewiseSEM' (Lefcheck,
317 2016).

To assess composite trait-climate relationships at both species- and community-level, we applied double constrained correspondence analysis (dc-CA; ter Braak et al., 2018). The dc-CA method is a new and powerful regression-based approach, similar to the covariance-based three-table ordination RLQ method used to assess multivariate trait-environment relationships in what is known as the fourth-corner problem (Dray & Legendre, 2008). Like RLQ, dc-CA uses three data tables (trait values of species, environmental conditions of sites, and abundances of species per site) to define the correlation between traits and environmental conditions (i.e., the fourth-corner correlation). The fourth-corner correlation has proved to be powerful to test trait-environment relationships (Peres-Neto et al, 2017; ter Braak 2017). dc-CA searches for linear combinations of traits and environmental variables that maximize their fourth-corner correlation, using weighted least-squares, where the weights for species and for sites are their total abundance. In contrast, RLQ maximizes covariance not correlation. By maximizing the fourth-corner correlation, dc-CA considers the influence of environmental conditions on community functional composition (i.e., CWM traits) in combination with how species (environmental) niche centroids (SNC) relate to their traits (ter Braak et al., 2018). SNCs represent the mean climatic conditions where species are found (weighted by abundances) and are related to species' traits to discover whether trait-mediated mechanisms influence species' distributions. Specifically, the SNC with respect to environmental variable **e** is a weighted mean, calculated as $u_j = \sum_{i=1}^{n} y_{ij} e_i / \sum_{i=1}^{n} y_{ij}$, where $y_{ij}$ refers to the abundance of the $j^{th}$ species in the $i^{th}$ site, and $e_i$ is the value of the environmental variable at the $i^{th}$ site.

We additionally applied dc-CA considering geographic gradients (latitude, longitude and degrees from equator) instead of climate variables as predictors, and performed variation partitioning to define the separate and shared effects of geographical and climatic gradients. We

used the dc-CA based max-test to check significance of the dc-CA axes (ter Braak et al., 2017). The max-test solves the problem of inflated type I error rate in the fourth-corner approach (Peres-Neto et al, 2017) by applying two independent permutations for testing species- (SNC ~ traits) and community-level (CWM ~ climate) patterns, and selecting the highest p-value. We applied the max-test after aggregating plots separated by less than 50 km (Fig. S5) to avoid pseudo-replication caused by nearby plots. In the analyses using dc-CA, the issue of the two exceptionally wet sites was solved by replacing their MAP values with the value 4500 mm/year, slightly higher than the maximum in the data set; this gave a slightly higher fit than the log-transformation, but did not give qualitatively different results. We performed the dc-CA using the software Canoco 5.12 (ter Braak & Šmilauer, 2018).

## Results

*Functional composition of Neotropical moist forest regions*

The functional composition of tree species pools largely overlapped across regions (Fig. 2a), but strong differences among regions emerged from abundance-weighted trait values at the local community-level (i.e., CWM) (Fig. 2b). Tree communities in forests near the equator (e.g., Amazonia, Northeastern Atlantic forest) were dominated by taller species with larger seeds, harder woods and greater leaf dry matter content. Tree communities in regions further from the equator were dominated by lower-statured species with smaller seeds and lower LDMC, particularly in the northern hemisphere (Fig. 2b). CWM values of wood density and maximum height were, however, relatively high at the extreme south (i.e., southeastern Atlantic forests), where specific leaf area achieved the lowest values (Fig. 2b).

The first two principal component axes of species-level trait values captured 55% of the variation in the functional space composed by six traits (Fig. 3a). The first PC axis indicated a common spectrum of variation among economic- and regenerative-traits, varying from species with acquisitive traits (i.e., high SLA, low LDMC and WD) and small seeds (i.e., opportunistic strategies), to species with more conservative strategies (i.e., low SLA, high LDMC and WD) and larger seeds (Fig. 3a, Table S5). The second axis mainly reflects variation in leaf area and maximum height, which co-varied positively (Fig. 3a, Table S5). Variation in SLA was mostly captured by a third PC axis (Table S5).

The first two principal components of community-level trait values (i.e., CWM) captured more variation (74%) and revealed similar trade-offs (Fig. 3b), except maximum height was strongly related to the first PC axis (Table S5). Tree communities from different regions could be distinguished along the first two PC axes (Fig. 3b). Specifically, the first axis indicated a gradient from communities dominated by species with conservative traits (high WD and LDMC) in equatorial regions and in the extreme south of the Neotropical forest biome, to a more acquisitive (high SLA) community composition in Northern forests. In turn, the second community trait axis distinguished communities at the Southeastern Atlantic region and Caribbean Islands as dominated by species with smaller leaves compared to more equatorial forests, particularly those across North-Amazon and Southern Meso-America (Fig. 3b).

*Trait-climate relationships across Neotropical tree communities*

Current climate explained 16 to 57% of the variation in CWM trait values across Neotropical moist forests (Table 1a, Fig. 4). Temperature seasonality presented the strongest relationships with CWM traits, except for leaf area which was more strongly related to mean annual

386 precipitation, and SLA which was not responsive to climate variation (Table 1a). LDMC, SM,
387 WD and Hmax decreased with increasing temperature seasonality, while mean annual
388 temperature had similar (but much weaker) effects on the last three of these traits (Table 1a).
389 Additionally, increasing annual precipitation was associated with increased dominance of tree
390 species with lower wood density, larger organs and lower leaf dry matter content, while
391 precipitation seasonality was negatively related to seed mass (Table 1a). The species functional
392 strategies evident on the first two PC axes (Fig. 3a) also changed predictably in response to
393 climatic variables (Table 1b): PC1 (acquisitive to conservative resource economy) was strongly
394 negatively related to temperature seasonality, while PC2 (small to large plants and organs)
395 increased mainly with mean annual precipitation (Fig. 4).

396 The first two dc-CA axes revealed significant (max-test, P = 0.001) composite trait-climate
397 relationships (Fig. 5, Table S6). The first axis describes a gradient from environments with
398 relatively high seasonality in temperature and precipitation, combined with high annual
399 precipitation and potential evapotranspiration, to less seasonal climates, along which there was a
400 shift in dominance from shorter plants with relatively acquisitive traits and small seeds, to slow-
401 growing species with conservative traits and large seeds (Fig. 5a). This first axis separated
402 communities across Northern regions from those at more equatorial regions (Fig. 5b). The
403 second dc-CA axis was mostly explained by variation in MAP and PET, reflecting a gradient
404 from drier sites under high potential evapotranspiration to exceptionally wet sites (Fig. 5a). This
405 second gradient explained the variation in dominance from small-leaved species with high
406 woody density across southeastern Atlantic forests and Caribbean Islands, to large-leaved, soft-
407 wooded species in communities across northern regions, particularly the Chocó bioregion and
408 North-Western Amazon (Fig. 5b).

Climate variables were good predictors of taxonomic composition across communities (CCA eigenvalues of 0.8 and 0.7 for the first two axes), as well as of multivariate gradients in community abundance-weighted traits (46% of variance explained; Table S6). In turn, traits were weak predictors of the distribution of individual species abundances across communities, explaining only 4% of variation in species climate niche centroids (Table S6). Forward selection on climate variables revealed that three of the five climate variables (MAP, TS and PET) account for most variation in composite trait-climate gradients (Fig. S6).

*Geographic gradients in community functional composition*

All community weighted mean traits were significantly related to either latitude or degrees from equator. LA, LDMC, WD and SM decreased with increasing degrees from equator, while SLA increased and Hmax decreased with latitude (i.e., from southern to northern forests; Fig. S7). Latitude was more strongly related to vegetation patterns (i.e., taxonomic turnover across communities), while degrees from equator explained relatively more of functional variation (Table S7). Variance partitioning revealed unique and shared effects of geography and climate, combining to explain 66% of the variation in CWM trait values (Table 2). Most of this explained variation (39%) resulted from shared effects of geographical gradients and climate variables, though there were also unique effects of similar size from both climate (15%) and geography (12%) (Table 2).

**Discussion**

Species pools of Neotropical moist forest regions from southern Mexico to southern Brazil possess similar distributions of trait values. Long-term filters that can control for the functional

composition of regional species pools thus have little to no importance. In contrast, local tree communities are functionally structured along climatic and (bio)geographical gradients. Species assembly processes that govern local abundance of species in tree communities must have generated the documented functional dissimilarities. The novelty of our findings is that we found clear though complex trait-climate relationships across Neotropical moist forests, that are not simply driven by geography. The observed patterns suggest an increase in relative abundance of lower-statured, light-wooded and softer-leaved species bearing smaller seeds (i.e., opportunistic strategies) under more seasonal climates in communities further away from the equator, especially under wetter and warmer conditions across northern forests. In contrast, communities in more stable climates (mostly close to the equator) are dominated by species with large seeds and conservative traits (i.e., the typical functional profile of late-successional tree species). Trait-climate relationships at the species-level (i.e., Species Niche Centroids ~ traits) were also significant but weaker, suggesting either that changes in the abundance of dominant species are responsible for varying functional signatures across Neotropical forests, or that there is scope for improvement of the trait set. It is important to recognize that dominance of functional strategies differ between regions mainly due to local assembly processes related to climate rather than changes in species pools that would be the result of biogeographic history. This helps to understand how Neotropical forests may respond to climate change and other human-imposed disturbances.

Our results contrast with those of Bruelheide et al. (2018), in which functional composition of plant communities (abundance-based) was weakly related to climate at the global scale. At the continental/biome scale (i.e., within Neotropics), we found strong trait-climate relationships across Neotropical moist forest tree communities, with combinations of climatic variables

455 explaining up to 57% of variance in CWM trait values. Changes in trait dominance were mainly
456 driven by the increase in temperature seasonality with distance from the equator and, to a lesser
457 extent, by changes in precipitation regimes, average temperature and potential evapotranspiration
458 (Table 1) that are less clear in geographic terms (Fig. 1). Slightly different from our findings,
459 previous assessments of global trait distributions suggest that higher mean annual temperature
460 and/or precipitation in equatorial regions leads to increased prevalence of conservative traits and
461 larger seeds (e.g., Swenson et al., 2012; Moles et al., 2014; Bruelheide et al., 2018). This
462 discrepancy may arise because global patterns of trait distribution may reflect major differences
463 among predominant biomes across climatic zones. Also, global-scale studies usually include
464 both woody and herbaceous species (e.g., Bruelheide et al., 2018), which respond differently to
465 climate across the Neotropics (Šímová et al., 2018). Most importantly, global-scale studies
466 include dry forests, where the combination of high temperatures with low and highly seasonal
467 precipitation may represent a physical stress, favoring conservative strategies (Westoby et al.,
468 2002). As our study focuses on Neotropical moist forests, higher temperatures and precipitation
469 should actually favor acquisitive traits of trees, as we found, due for example to increased
470 hydraulic efficiency (Zhang et al., 2013; Santiago et al., 2018). Our findings strengthen the
471 notion that climatic conditions play a key role in trait filtering across Neotropical tree
472 assemblages.

473 Despite differences in magnitude of climate effects, the direction of community-level trait-
474 climate relationship (i.e., including abundance data) in the Neotropics generally agrees with that
475 of species-level global trait-climate relationships (e.g., Swenson et al., 2012; Wright et al., 2017,
476 see Moles, 2018 for a review of these relationships). For example, we found that seed mass tends
477 to be lower in plants growing at more seasonal sites further from the equator, as observed

elsewhere (Moles et al., 2007; Swenson et al., 2012; Malhado et al., 2015), presumably because larger seeds require longer growing seasons for development and are less likely to exhibit dormancy that helps to survive under adverse seasonal conditions (Thompson et al., 1993; de Casas et al., 2017). Moreover, tree species in wetter sites tend to present larger leaves and softer wood and leaf tissues, as we found, because these traits maximize resource capture in productive environments (Westoby et al., 2002; Wright et al., 2017). Conversely, small leaves with low specific leaf area (SLA) characterize cold tolerance (Poorter et al., 2009; Wright et al., 2017) as we observed in the southeastern Atlantic forests, a region that experiences relatively low and seasonal temperatures (Fig. S1; Oliveira-Filho et al., 2013). Also in agreement with our findings, plant height tends to be limited under more seasonal climates (Moles et al., 2009; Swenson et al., 2012), and non-significant relationships between SLA and climatic gradients is more a rule than an exception (Moles, 2018). Finally, large seeds and conservative traits may provide advantages for species in shaded conditions of relatively closed-canopy forests near the equator (Leishman & Westoby, 1994; Kitajima & Poorter, 2010).

While trait-climate relationships we observed are well supported by theory, they might to some extent be driven by (bio)geography, as some climatic variables were strongly correlated to either latitude or distance from equator. For instance, temperature seasonality increases sharply with distance to equator ($R^2 = 0.81$), which similarly explain community functional composition (*cf.*, Figs. 4 and S7). We can thus only speculate about the relative importance of climatic and geographic gradients, as they share the largest fraction of explained variance in CWM traits. However, we note that both climate and geography have also unique effects on community functional composition (Table 2). To illustrate this, the Southern Brazilian Atlantic forest does not fully follow the trend of increasing dominance of opportunistic strategies with distance from

equator, as it supports many large, hard-wooded trees. This can, however, be explained by combinations of climatic factors, given the seasonal but relatively cold and dry climates in the southern (compared to the northern) extreme of the Neotropics (Fig. S1), which select for conservative strategies. In fact, most species in this southernmost region have tropical-subtropical ranges due to forest expansion over subtropical grasslands during the last glacial maximum (Oliveira-Filho et al., 2013; Costa et al., 2017). Also, the dominance of species with small leaves and conservative traits under wet and warm climates in the Caribbean region deviates from the trait-climate relationships, but may reflect selection by hurricane-force winds for stronger structural support (Lugo, 2000).

There is a consensus that climate change will make tropical forests warmer, with more seasonal rainfall and temperature including more frequent droughts, more heavy rains and frequent heatwaves (IPCC, 2014). These are conditions currently found across northern Neotropical moist forest regions, where opportunistic strategies thrive. Therefore, it is reasonable to expect forests in northern Neotropical regions to be more resilient to predicted climate changes, unless climate change leads to drastic changes towards alternative ecosystem states, like dry forest or woodlands. In contrast, climate changes should lead southern and especially equatorial forests of the future to more closely resemble the today's northern Neotropical moist forests due to proliferation of opportunistic strategies already present in regional species pools (Fig. 2a). This can disrupt ecosystem services such as carbon sequestration and storage if forests once dominated by conservative traits experience the proliferation of more opportunistic strategies (Poorter et al., 2017), including soft-wooded species that grow fast but die young (Brienen et al., 2020).

In summary, tree communities across Neotropical moist forests are functionally distinct because particular traits are favored under particular climates. Such functional predictability permits insights into tropical forest responses to global changes and the consequences for biodiversity persistence, provision of ecosystem services and global sustainability (Díaz et al., 2007). In fact, as ecosystem functioning is determined by the dominant traits in tropical forests (Poorter et al., 2017), our findings can help to anticipate the impact of future climate change and/or human-induced disturbances (e.g., habitat loss, fragmentation) on the functioning of Neotropical forests. For instance, we must expect an increase in prevalence of low-statured tree species with relatively acquisitive traits and small seeds, based on scenarios of increasing climate seasonality (IPCC, 2014). This functional strategy is associated with faster growth and reproductive rates (Reich, 2014; Moles, 2018) and thrives in human-modified tropical landscapes worldwide (Laurance et al., 2006; Santos et al., 2008), but plays a limited role in crucial ecosystem services such as carbon and nutrient retention (Poorter et al., 2017). Overall, this changing functional structure of Neotropical moist forests is likely to confer varying degrees of resilience to human-caused disturbances. Neotropical moist forests vary widely in functional terms and one should be aware of these differences when it comes to understand the functional assembly of Neotropical tree communities.

**Acknowledgements**

This study was carried out with the financial support of the Coordenação de Aperfeiçoamento de Pessoal de Nivel Superior – Brasil (CAPES) – Finance code 001; and the Conselho Nacional de Desenvolvimento Científico e Tecnológico – CNPQ (grant 403770/2012-2). BXP was funded by a PhD scholarship from CNPq (140260/2015-3). BXP collected functional data in the Mexican

regions with the financial support of the Catedra José Sarukhán and the Centro del Cambio Global y la Sustentabilidad en el Sureste. BXP finished this study with the support of a postdoctoral fellowship from Fundação de Amparo à Ciência e Tecnologia do Estado de Pernambuco (FACEPE). FPLM, MT and BAS thank CNPq for productivity grants.

## Data Accessibility

Data and R codes used for the analyses are available from the Dryad Digital Repository: http://doi.org/10.5061/dryad.vq83bk3s3. The dc-CA variation decomposition with statistical tests of Table 2 is available at https://doi.org/10.6084/m9.figshare.13259534.v2

## Authorship

BXP, MT and FPLM conceived the ideas and designed methodology; BXP collected, compiled and analysed the data, with the supervision of CtB on the dc-CA analysis; BXP wrote the first draft with significant contribution from FPLM. All authors contributed data and/or with critical insights that improved the manuscript.

## References

Arroyo-Rodríguez, V., Pineda, E., Escobar, F., & Benítez-Malvido, J. (2009). Value of small patches in the conservation of plant-species diversity in highly fragmented rainforest. *Conservation Biology*, 23, 729-739.

Balmford, A. (1996). Extinction filters and current resilience: the significance of past selection pressures for conservation biology. Trends in Ecology and Evolution, 11, 193-196.

568 Barton, K. (2014). MuMin: Multi-model inference. R package version 1.10.0. https://cran.r-
569 project.org/web/packages/MuMIn/index.html
570 Bates, D., Maechler, M., Bolker, B., & Walker, S. (2015). Fitting Linear Mixed-Effects Models
571 Using lme4. *Journal of Statistical Software*, 67, 1-48.
572 Benchimol, M., & Peres, C. A. (2015). Edge-mediated compositional and functional decay of
573 tree assemblages in Amazonian forest islands after 26 years of isolation. *Journal of*
574 *Ecology*, 103, 408–420.
575 Betts, M. G., Wolf, C., Pfeifer, M., Banks-Leite, C., Arroyo-Rodríguez, V., … Ewers, R. M.
576 (2019). Extinction filters mediate the global effects of habitat fragmentation on animals.
577 *Science*, 366, 1236-1239.
578 Blonder, B., Enquist, B. J., Graae, B. J., Kattge, J., Maitner, B. S., Morueta-Holme, N., ... Violle,
579 C. (2018). Late Quaternary climate legacies in contemporary plant functional composition.
580 *Global Change Biology*, 24, 4827-4840.
581 Brienen, R. J. W., Caldwell, L., Duchesne, L., Voelker, S., Barichivich, J., Baliva, M., … Gloor,
582 E. (2020). Forest carbon sink neutralized by pervasive growth-lifespan trade-offs. *Nature*
583 *Communications*, 11, 4241.
584 Brown, J. H. (2014). Why are there so many species in the tropics? *Journal of Biogeography*, 41,
585 8-22.
586 Bruelheide, H., Dengler, J., Purschke, O., Lenoir, J., Jiménez-Alfaro, B., Hennekens, S. M., ...
587 Jandt, U. (2018). Global trait–environment relationships of plant communities. *Nature*
588 *Ecology & Evolution*, 2, 1906-1917.
589 Brum, M., Vadeboncoeur, M. A., Ivanov, V., Asbjornsen, H., Saleska, S., … Oliveira, R.S.
590 (2019). Hydrological niche segregation defines forest structure and drought tolerance

591 strategies in a seasonal Amazon forest. *Journal of Ecology*, 107, 318-333.
592 Burnham, R. J., & Graham, A. (1999). The History of Neotropical Vegetation: New
593 Developments and Status. *Annals of the Missouri Botanical Garden*, 86, 546-589.
594 Cadotte, M. W., & Tucker, C. M. (2017). Should environmental filtering be abandoned? *Trends*
595 *in Ecology and Evolution*, 32, 429-437.
596 Cole, L. E. S., Bhagwat, S. A., & Willis, K. J. (2014). Recovery and resilience of tropical forests
597 after disturbance. *Nature Communications*, 5, 3906.
598 Colinvaux, P. A., De Oliveira, P. E., & Bush, M. B. (2000). Amazonian and neotropical plant
599 communities on glacial time-scales: The failure of the aridity and refuge hypotheses.
600 *Quaternary Science Reviews*, 19, 141–169.
601 de Casas, R., Willis, C. G., Pearse, W. D., Baskin, C. C., Baskin, J. M., & Cavender-Bares, J.
602 (2017). Global biogeography of seed dormancy is determined by seasonality and seed size:
603 A case study in the legumes. *New Phytologist*, 214, 1527–1536.
604 Díaz, S., Kattge, J., Cornelissen, J. H. C., Wright, I. J., Lavorel, S., Dray, S., … Gorné, L. D.
605 (2016). The global spectrum of plant form and function. *Nature*, 529, 167–171.
606 Díaz, S., Lavorel, S., de Bello, F., Quétier, F., Grigulis, K., Robson, T. M. (2007). Incorporating
607 plant functional diversity effects in ecosystem service assessments. *Proceedings of the Na-*
608 *tional Academy of Sciences*, 104, 20684-20689.
609 Dray, S., & Legendre, P. (2008). Testing the species traits–environment relationships: the fourth-
610 corner problem revisited. *Ecology*, 89, 3400-3412.
611 Faria, D., Mariano-Neto, E., Martini, A. M. Z., Ortiz, J. V., Montingelli, R., Rosso, S., ...
612 Baumgarten, J. (2009). Forest structure in a mosaic of rainforest sites: The effect of

613 fragmentation and recovery after clear cut. *Forest Ecology and Management*, 257, 2226–
614 2234.
615 Fick, S. E., & Hijmans, R. J. (2017). Worldclim 2: New 1-km spatial resolution climate surfaces
616 for global land areas. *International Journal of Climatology*, 37, 4302-4315.
617 Frierson, D., Hwang, Y., Fučkar, N., Seager, R., Kang, S. M., Donohoe, A., Battisti, D. S.
618 (2013). Contribution of ocean overturning circulation to tropical rainfall peak in the
619 Northern Hemisphere. *Nature Geoscience*, 6, 940–944.
620 Fukami, T. (2015). Historical contingency in community assembly: integrating niches, species
621 pools, and priority effects. *Annual Review of Ecology, Evolution, and Systematics*, 46, 1-
622 23.
623 Gentry, A. H. (1982). Neotropical Floristic Diversity: Phytogeographical Connections Between
624 Central and South America, Pleistocene Climatic Fluctuations, or an Accident of the
625 Andean Orogeny? *Annals of the Missouri Botanic Garden*, 69, 557-593.
626 Gentry, A. H. (1988). Changes in plant community diversity and floristic composition on
627 environmental and geographical gradients. *Annals of the Missouri Botanic Garden*, 75, 1-
628 34.
629 Graham, A. (1999). The Tertiary History of the Northern Temperate Element in the Northern
630 Latin American Biota. *American Journal of Botany*, 86, 32-38.
631 Grime, J. P., & Pierce, S. (2012). The Evolutionary Strategies that Shape Ecosystems. Wiley-
632 Blackwell, Chichester, UK.
633 Hernández-Ruedas, M. A., Arroyo-Rodríguez, V., Meave, J. A., Martínez-Ramos, M., Ibarra-
634 Manríquez, G., Martínez, E., … Santos, B.A. (2014). Conserving tropical tree diversity and

635 forest structure: The value of small rainforest patches in moderately-managed landscapes.
636 *PLoS ONE*, 9, e98931.
637 IPCC (2014). *Climate Change 2014: Synthesis Report. Contribution of Working Groups I, II and*
638 *III to the Fifth Assessment Report of the Intergovernmental Panel on Climate Change*
639 [Core Writing Team, R.K. Pachauri and L.A. Meyer (eds.)]. IPCC, Geneva, Switzerland
640 Kattge, J., Bönisch, G., Díaz, S., Lavorel, S., Prentice, I. C., … Wirth, C. (2020). TRY plant trait
641 database – enhanced coverage and open access. *Global Change Biology*, 26, 119–188.
642 Kikuzawa, K., Onoda, Y., Wright, I. J., & Reich, P. B. (2013). Mechanism of leaf longevity
643 patterns. *Global Ecology and Biogeography*, 22, 982-993.
644 Kitajima, K., & Poorter, L. (2010). Tissue-level leaf toughness, but not lamina thickness,
645 predicts sapling leaf lifespan and shade tolerance of tropical tree species. *New Phytologist*,
646 186, 708-721.
647 Kobe, R. K. (1999). Light gradient partitioning among tropical tree species through differential
648 seedling mortality and growth. Ecology, 80, 187-201.
649 Kraft, N. J. B., & Ackerly, D. D. (2014). Assembly of Plant Communities. In: Monson R.
650 (eds) *Ecology and the Environment*. The Plant Sciences, vol 8. Springer, New York.
651 Laliberté, E., & Legendre, P. (2010). A distance-based framework for measuring functional
652 diversity from multiple traits. *Ecology*, 91, 2099–3005.
653 Laurance, W. F., Nascimento, H. E. M., Laurance, S. G., Andrade, A. C., Fearnside, P. M.,
654 Ribeiro, J. E. L., & Capretz, R. L. (2006). Rain forest fragmentation and the proliferation
655 of successional trees. *Ecology*, 87, 469–482.
656 Lefcheck, J. S. (2016). piecewiseSEM: Piecewise structural equation modeling in R for ecology,
657 evolution, and systematics. *Methods in Ecology and Evolution*, 7, 573-579.

Leishman, M. R., & Westoby, M. (1994). The role of large seed size in shaded conditions – Experimental evidence. *Functional Ecology*, 8, 205–214.

Leite, Y. L. R., Costa, L., Loss, A. C., Rocha, R. G., Batalha-Filho, H., Bastos, A., & Pardini, R. (2016). Neotropical forest expansion during the last glacial period challenges refuge hypothesis. *Proceedings of the National Academy of Sciences of the United States of America*, 113, 1008-1013.

Maitner, B. S., Boyle, B., Casler, N., Condit, R., Donoghue II, J., Durán, S. M., ... Enquist, B. J. (2018). The BIEN R package: A tool to access the Botanical Information and Ecology Network (BIEN) Database. *Methods in Ecology and Evolution*, 9, 373–379.

Malhado, A., Oliveira-Neto, J. A., Stropp, J., Strona, G., Dias, L. C., Pinto, L. B., & Ladle, R. J. (2015). Climatological correlates of seed size in Amazonian forest trees. *Journal of Vegetation Science*, 26, 956–963.

Mittelbach, G. G., & Schemske, D. W. (2015). Ecological and evolutionary perspectives on community assembly. *Trends in Ecology and Evolution*, 30, 241 – 247.

Moles, A. T. (2018). Being John Harper: Using evolutionary ideas to improve understanding of global patterns in plant traits. *Journal of Ecology*, 106, 1-18.

Moles, A. T., Ackerly, D. D., Tweddle, J. C., Dickie, J. B., Smith, R., Leishman, M. R., … Westoby, M. (2007). Global patterns in seed size. *Global Ecology and Biogeography*, 16, 109-116.

Moles, A. T., Perkins, S. E., Laffan, S. W., Flores-Moreno, H., Awasthy, M., Tindall, M. L., ... Bonser, S.P. (2014). Which is a better predictor of plant traits: temperature or precipitation? *Journal of Vegetation Science*, 25, 1167–1180.

Moles, A. T., Warton, D. I., Warman, L., Swenson, N. G., Laffan, S. W., Zanne, A. E., … Leishman, M.R. (2009). Global patterns in plant height. *Journal of Ecology*, 97, 923–932.

Mora, C., Frazier, A., Longman, R., Dacks, R. S., Walton, M. M., Tong, E. J., … Giambelluca, T. W. (2013). The projected timing of climate departure from recent variability. *Nature*, 502, 183-187.

Morueta-Holme, N., Enquist, B. J., McGill, B. J., Boyle, B., Jørgensen, P. M., Ott, J.E., … Svenning, J-C. (2013). Habitat area and climate stability determine geographical variation in plant species range sizes. *Ecology Letters*, 16, 1446–1454.

Muller-Landau, H. C. (2010). The tolerance-fecundity trade-off and the maintenance of diversity in seed size. *Proceedings of the National Academy of Sciences of the United States of America*, 107, 4242-4247.

Muscarella, R., Lohbeck, M., Martínez-Ramos, M., Poorter, L., Rodríguez-Velázquez, J. E., van Breugel, M., & Bongers, F. (2017). Demographic drivers of functional composition dynamics. *Ecology*, 98, 2743-2750.

Nakagawa, S., & Schielzeth, H. (2013). A general and simple method for obtaining R2 from generalized linear mixed-effects models. *Methods in Ecology and Evolution*, 4, 133–142.

Neter, J., Kutner, M.H., Nachtsheim, C.J., & Wasserman, W. (1996). Applied linear statistical models. – McGraw- Hill/Irwin.

Oliveira-Filho, A. T., Budke, J. C., Jarenkow, J. A., Eisenlohr, P. V., Neves, D. R. M. (2013). Delving into the variations in tree species composition and richness across South American subtropical Atlantic and Pampean forests. *Journal of Plant Ecology*, 8, 242–260.

Orihuela, R. L. Z., Peres, C. A., Mendes, G., Jarencow, J. A., & Tabarelli, M. (2015). Markedly divergent tree assemblage responses to tropical forest loss and fragmentation across a strong seasonality gradient. *PLoS One*, 10, e0136018

Peres-Neto, P. R., Dray, S., & ter Braak, C. J. F. (2017). Linking trait variation to the environment: critical issues with community-weighted mean correlation resolved by the fourth-corner approach. *Ecography*, 40, 806-816.

Pérez-Harguindeguy, N., Díaz, S., Garnier, E., Lavorel, S., Poorter, H., Jaureguiberry, P., … Cornelissen, J. H. C. (2013). New handbook for standardised measurement of plant functional traits worldwide. *Australian Journal of Botany*, 61, 167–234.

Pierce, S., Negreiros, D., Cerabolini, B. E. L., Kattge, J., Díaz, S., Kleyer, M., … Tampucci, D. (2017). A global method for calculating plant CSR ecological strategies applied across biomes world-wide. *Functional Ecology*, 31, 444–457.

Pinho, B. X., de Melo, F. P. L., Arroyo-Rodríguez, V., Pierce, S., Lohbeck, M., & Tabarelli, M. (2018). Soil-mediated filtering organizes tree assemblages in regenerating tropical forests. *Journal of Ecology*, 106, 137–147.

Pitman, N. C. A., Terborgh, J. W., Silman, M. R., Núñez, V. P., Neill, D. A., Cerón, C. E., Palacios, W.A., & Aulestia, M. (2001). Dominance and distribution of tree species in upper Amazonian terra firme forests. *Ecology*, 82, 2101-2117.

Poorter, H., Niinemets, Ü., Poorter, L., Wright, I. J., & Villar, R. (2009). Causes and consequences of variation in leaf mass per area (LMA): a meta-analysis. *New Phytologist*, 182, 565–588.

Poorter, L., van der Sande, M. T., Arets, E. J. M. M., Ascarrunz, N., Enquist, B., Finegan, B., ... Peña-Claros, M. (2017). Biodiversity and climate determine the functioning of Neotropical

forests. *Global Ecology and Biogeography*, 26, 1423–1434.

Reich, P. B. (2014). The world-wide 'fast-slow' plant economics spectrum: a traits manifesto. *Journal of Ecology*, 102, 275–301.

Royal Botanic Gardens Kew (2020). Seed Information Database (SID). Version 7.1. Available from: http://data.kew.org/sid/

Santiago, L. S., De Guzman, M. E., Baraloto, C., Vogenberg, J. E., Brodie, M., Hérault, B., Fortunel, C., & Bonal, D. (2018). Coordination and trade-offs among hydraulic safety, efficiency and drought avoidance traits in Amazonian rainforest canopy tree species. *New Phytologist*, 218, 1015-1024.

Sandel, B., Weigelt, P., Kreft, H., Keppel, G., van der Sande, M. T., Levin, S., Smith, S., Craven, D., & Knight, T. M. (2020). Current climate, isolation and history drive global patterns of tree phylogenetic endemism. *Global Ecology and Biogeography*; 29, 4-15.

Santos, B. A., Peres, C. A., Oliveira, M. A., Grillo, A., Alves-Costa, C. P., & Tabarelli, M. (2008). Drastic erosion in functional attributes of tree assemblages in Atlantic forest fragments of northeastern Brazil. *Biological Conservation*, 141, 249–260.

Siefert, A., Violle, C., Chalmandrier, L., Albert, C. H., Taudiere, A., Fajardo, A., … Wardle, D. A. (2015). A global meta-analysis of the relative extent of intraspecific trait variation in plant communities. *Ecology Letters*, 18, 1406–1419.

Šímová, I, Violle, C, Svenning, J-C, Kattge, J., Engemann, K., Sandel, B., ... Enquist, B.J. (2018). Spatial patterns and climate relationships of major plant traits in the New World differ between woody and herbaceous species. *Journal of Biogeography*, 45, 895-916.

Swenson, N. G., & Enquist, B. J. (2007). Ecological and evolutionary determinants of a key plant functional trait: Wood density and its community-wide variation across latitude and elevation. *American Journal of Botany*, 94, 451–459.

Swenson, N. G., Enquist, B. J., Pither, J., Kerkhoff, A. J., Boyle, B., Weiser, M. D., … Nolting, K. (2012). The biogeography and filtering of woody plant functional diversity in North and South America. *Global Ecology and Biogeography*, 21, 798–808.

ter Braak, C. J. F. (2017). Fourth-corner correlation is a score test statistic in a log-linear trait–environment model that is useful in permutation testing. *Environmental and Ecological Statistics*, 24**,** 219–242.

ter Braak, C. J. F., & Šmilauer, P. (2018). *Canoco reference manual and user's guide: software for ordination* (version 5.10). Microcomputer Power, Ithaca, USA, 536 pp.

ter Braak, C. J. F., Šmilauer, P., & Dray, S. (2018). Algorithms and biplots for double constrained correspondence analysis. *Environmental and Ecological Statistics*, 25, 171-197.

Thompson, K., Band, S. R., & Hodgson, J. G. (1993). Seed size and shape predict persistence in the soil. *Functional Ecology*, 7, 236-241.

Trabucco, A., & Zomer, R. J. (2018). Global Aridity Index and Potential Evapo-Transpiration (ET0) Climate Database v2. CGIAR Consortium for Spatial Information (CGIAR-CSI). Published online, available from the CGIAR-CSI GeoPortal at https://cgiarcsi.community

van Buuren, S., & Groothuis-Oudshoorn, K. (2011). mice: Multivariate Imputation by Chained Equations in R. *Journal of Statistical Software*, 45, 1-67.

van der Sande, M., Arets, E., Peña-Claros, M., De Avila, A., Roopsind, A., Mazzei, L., ... Poorter, L. (2016). Old-growth Neotropical forests are shifting in species and trait composition. *Ecological Monographs*, 86, 228-243.

Venables, W. N., & Ripley, B. D. (2002). *Modern Applied Statistics with S*, Springer-Verlag.

Violle, C., Reich, P. B., Pacala, S. W., Enquist, B. J., & Kattge, J. (2014). The emergence and promise of functional biogeography. *Proceedings of the National Academy of Sciences of the United States of America*, 111, 13690–13696.

Westoby, M., Falster, D. S., Moles, A. T., Vesk, P. A., & Wright, I. J. (2002). Plant Ecological Strategies: Some Leading Dimensions of Variation Between Species. *Annual Review of Ecology and Systematics*, 33, 125–159.

Wright, I. J., Dong, N., Maire, V., Prentice, I. C., Westoby, M., Díaz, S., ... Wilf, P. (2017). Global climatic drivers of leaf size. *Science*, 357, 917–921.

Wright, S. J., Muller-Landau, H. C., & Schipper, J. (2009). The Future of Tropical Species on a Warmer Planet. *Conservation Biology*, 23, 1418-1426.

Wright, I. J., Reich, P. B., Westoby, M., Ackerly, D. D., Baruch, Z., Bongers, F., …, Villar, R. (2004). The world-wide leaf economics spectrum. *Nature*, 428, 821–827.

Zhang, S. B., Cao, K. F., Fan, Z. X., & Zhang, J. L. (2013). Potential hydraulic efficiency in angiosperm trees increases with growth-site temperature but has no trade-off with mechanical strength. *Global Ecology and Biogeography*, 22, 971–981.

785 **Table 1.** Results of averaging of the best-fitted mixed-effects models (ΔAICc< 2) analysing the effects of climatic variables on the
786 abundance-weighted community mean of (a) functional traits and (b) functional strategies, across 471 forest plots in nine
787 biogeographic regions distributed throughout the Neotropics (see Fig. 1). For each variable retained in a best-fit model, we indicated
788 the mean coefficient (β), the standard error (SE), the 95% confidence intervals (95% CI) and the *p*-value. P-values of significant
789 variables (according to 95% confidence intervals) are in bold. The predictors were standardized and thus the coefficients indicate their
790 relative contribution for each response variable. The marginal $R^2$ (variance explained by climatic factors) and conditional $R^2$ (the
791 former plus additional among-regions variance not explained by climatic factors) values of the full model are also shown. Units of
792 climatic variables: MAP (mm), PET (mm), MAT (ºC), PS (coefficient of variation of monthly values), TS (standard deviation of
793 monthly values multiplied by 100).

| Model factors | β | SE | 95% CI | | p-value | Models R2 (marginal/conditional) |
|---|---|---|---|---|---|---|
| | | | Lower | Upper | | |
| **(a) Functional traits** | | | | | | |
| **Log (leaf area [cm²])** | | | | | | 0.24/0.29 |
| Annual precipitation (MAP) | 0.096 | 0.017 | 0.062 | 0.130 | **<2e-16** | |
| Potential evapotranspiration (PET) | -0.124 | 0.024 | -0.171 | -0.076 | **4.00E-07** | |
| Annual temperature (MAT) | 0.059 | 0.026 | 0.008 | 0.109 | **0.023** | |

| | | | | | | |
|---|---|---|---|---|---|---|
| Precipitation seasonality (PS) | 0.043 | 0.028 | 0.015 | 0.092 | 0.126 | |
| Temperature seasonality (TS) | 0.024 | 0.031 | -0.016 | 0.102 | 0.443 | |
| **Log (specific leaf area [cm²/g])** | | | | | | 0.09/0.32 |
| Annual precipitation (MAP) | 0.010 | 0.007 | 0.000 | 0.024 | 0.160 | |
| Annual temperature (MAT) | 0.010 | 0.007 | -0.001 | 0.025 | 0.155 | |
| Precipitation seasonality (PS) | 0.010 | 0.010 | 0.000 | 0.030 | 0.284 | |
| Potential evapotranspiration (PET) | -0.001 | 0.005 | -0.029 | 0.011 | 0.795 | |
| Temperature seasonality (TS) | -0.003 | 0.007 | -0.030 | 0.009 | 0.695 | |
| **Leaf dry matter content (g/g)** | | | | | | 0.47/0.70 |
| Temperature seasonality (TS) | -0.025 | 0.003 | -0.031 | -0.020 | **<2e-16** | |
| Annual precipitation (MAP) | -0.003 | 0.002 | -0.006 | 0.000 | **0.026** | |
| Annual temperature (MAT) | -0.003 | 0.003 | -0.008 | 0.000 | 0.224 | |
| Potential evapotranspiration (PET) | -0.002 | 0.003 | -0.010 | 0.003 | 0.576 | |
| Precipitation seasonality (PS) | 0.0001 | 0.001 | -0.005 | 0.004 | 0.894 | |
| **Log (seed mass [mg]+1)** | | | | | | 0.57/0.68 |
| Temperature seasonality (TS) | -0.653 | 0.067 | -0.783 | -0.522 | **<2e-16** | |

| | | | | | | |
|---|---|---|---|---|---|---|
| Annual temperature (MAT) | -0.161 | 0.056 | -0.270 | -0.051 | **0.003** | |
| Precipitation seasonality (PS) | -0.107 | 0.047 | -0.188 | -0.016 | **0.022** | |
| Potential evapotranspiration (PET) | -0.032 | 0.058 | -0.220 | 0.035 | 0.577 | |
| Annual precipitation (MAP) | -0.003 | 0.017 | -0.088 | 0.062 | 0.869 | |
| **Wood density (g/cm³)** | | | | | | 0.39/0.62 |
| Temperature seasonality (TS) | -0.052 | 0.006 | -0.064 | -0.040 | **<2e-16** | |
| Annual precipitation (MAP) | -0.018 | 0.003 | -0.024 | -0.011 | **3.00E-07** | |
| Annual temperature (MAT) | -0.016 | 0.005 | -0.026 | -0.005 | **0.003** | |
| Potential evapotranspiration (PET) | 0.009 | 0.007 | 0.000 | 0.024 | 0.207 | |
| Precipitation seasonality (PS) | -0.003 | 0.005 | -0.016 | 0.001 | 0.523 | |
| **Sqrt (maximum height [m])** | | | | | | 0.16/0.41 |
| Temperature seasonality (TS) | -0.190 | 0.034 | -0.256 | -0.125 | **<2e-16** | |
| Annual temperature (MAT) | -0.173 | 0.033 | -0.239 | -0.108 | **2.00E-07** | |
| Potential evapotranspiration (PET) | 0.057 | 0.045 | 0.005 | 0.145 | 0.204 | |
| Precipitation seasonality (PS) | -0.004 | 0.014 | -0.065 | 0.030 | 0.767 | |

**(b) Functional strategies**

| | | | | | | |
|---|---|---|---|---|---|---|
| **PC1 (economics spectrum)** | | | | | | 0.40/0.69 |
| Annual precipitation (MAP) | -0.096 | 0.032 | 0.034 | 0.158 | **0.002** | |
| Annual temperature (MAT) | -0.159 | 0.043 | 0.075 | 0.243 | **0.0002** | |
| Temperature seasonality (TS) | -0.560 | 0.057 | 0.448 | 0.673 | **<2e-16** | |
| Precipitation seasonality (PS) | -0.017 | 0.035 | -0.033 | 0.140 | 0.634 | |
| Potential evapotranspiration (PET) | 0.013 | 0.037 | -0.174 | 0.068 | 0.739 | |
| **PC2 (size spectrum)** | | | | | | 0.28/0.28 |
| Annual precipitation (MAP) | 0.120 | 0.013 | -0.145 | -0.094 | **<2e-16** | |
| Potential evapotranspiration (PET) | -0.125 | 0.017 | 0.092 | 0.158 | **<2e-16** | |
| Precipitation seasonality (PS) | 0.060 | 0.015 | -0.090 | -0.031 | **7.15E-05** | |
| Temperature seasonality (TS) | -0.024 | 0.021 | 0.001 | 0.068 | 0.255 | |
| Annual temperature (MAT) | 0.022 | 0.023 | -0.073 | 0.002 | 0.325 | |

794

795 **Table 2.** Variation partitioning of the trait-structured variation in the dc-CA with all traits, showing the unique and shared effects of
796 geography (latitude, longitude, and degrees from equator) and climate (MAP, MAT, TS, PS, PET) in aggregated samples of tree
797 communities across Neotropical moist forests (N = 59; see Fig. S5). The trait-structured variation is a weighted variance of the CWMs
798 with respect to orthonormalized traits with the sample total as weight.

| Component | Variation (Adj R2) | % of Explained | DF | Mean Square | F | P |
|---|---|---|---|---|---|---|
| Climate (unique) | 0.15 | 22.7 | 5 | 0.03 | 5.9 | 0.0005 |
| Geography (unique) | 0.12 | 17.8 | 3 | 0.04 | 7.2 | 0.0045 |
| Shared | 0.39 | 59.5 | -- | -- | | -- |
| Total Explained | 0.66 | 100 | 8 | 0.09 | 15.3 | 0.0005 |

799

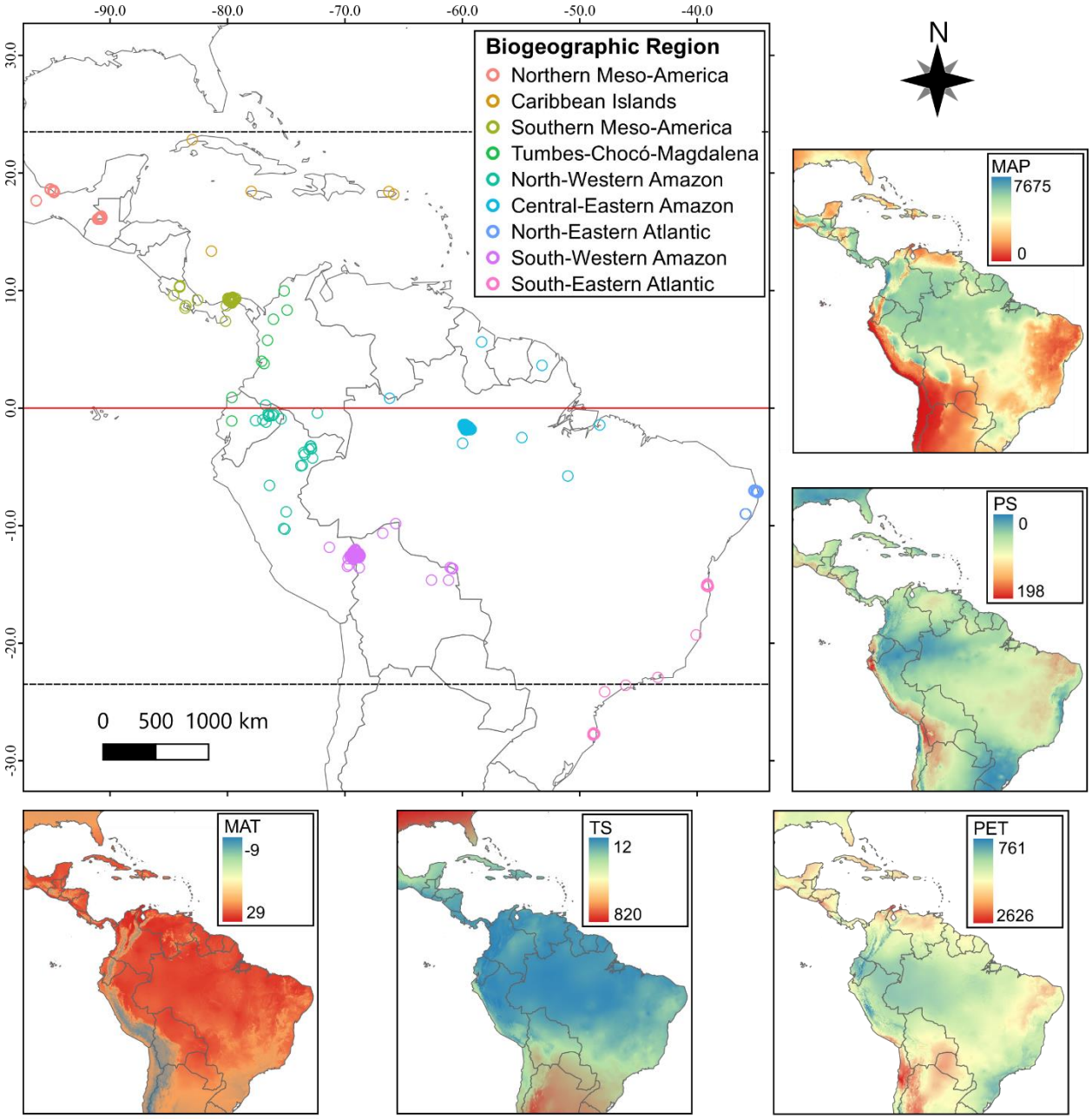


800

801 **Figure 1.** Location of the 471 forest plots studied in nine biogeographic regions, and variation in

802 the five climatic variables considered throughout the Neotropics. MAP, mean annual

803 precipitation (mm); MAT, mean annual temperature (ºC); PS, precipitation seasonality

804 (coefficient of variation of monthly precipitation values); TS, temperature seasonality (standard

805 deviation of monthly temperature values); PET, potential evapotranspiration (mm).

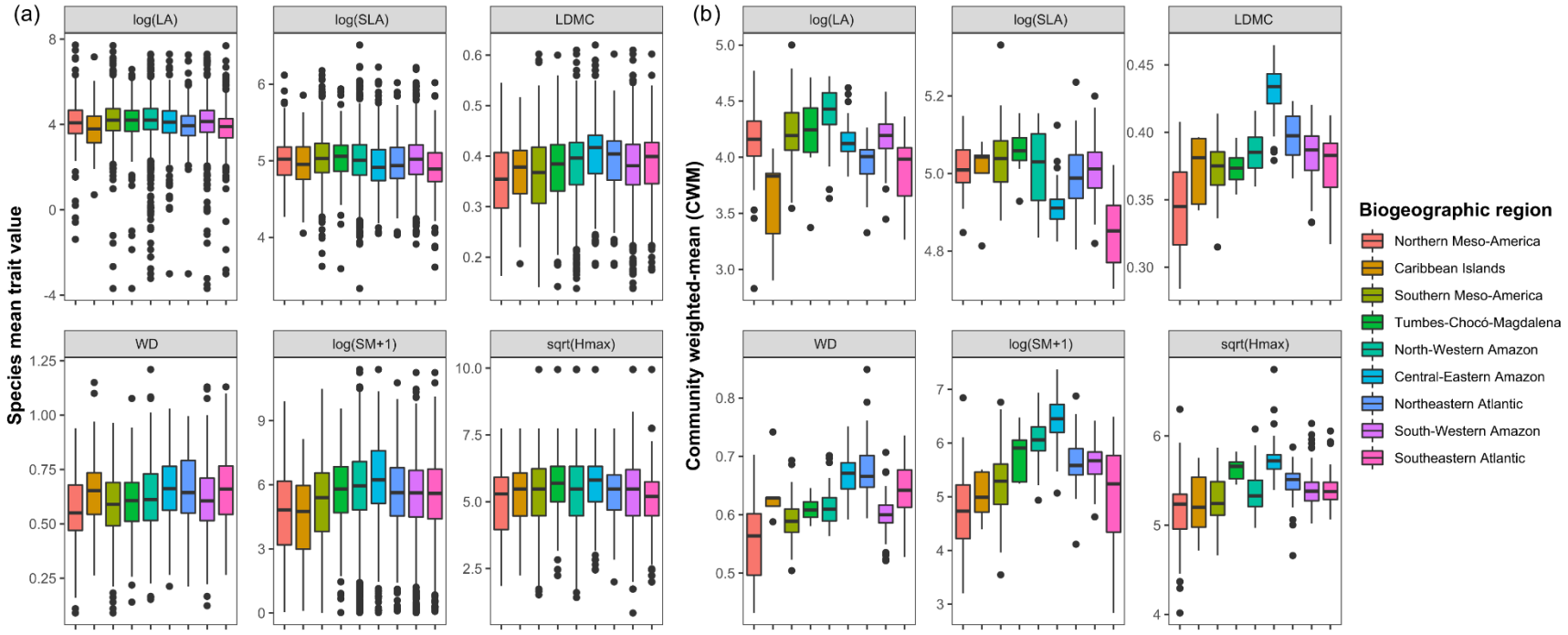


**Figure 2.** Differences between regions in functional trait values of (a) species present in each regional species pool (unweighted by abundance), and (b) the communities (i.e., abundance-weighted means – CWM) in each region, for 3,417 tree species distributed in 471 forest plots across nine Neotropical moist forest regions. Boxplots indicate the median (center line), 25-75% quartiles (box edges), < 1.5 times the inter quartile range (whiskers), and extreme values (dots). The boxplots are organized from the northernmost (left) to the southernmost region (right) along the distribution of the Neotropical moist forest biome. LA, leaf area ($cm^2$); SLA, specific leaf area ($cm^2/g$); LDMC, leaf dry matter content (g/g); WD, wood density ($g/cm^3$); SM, seed mass (mg); Hmax, maximum height (m).

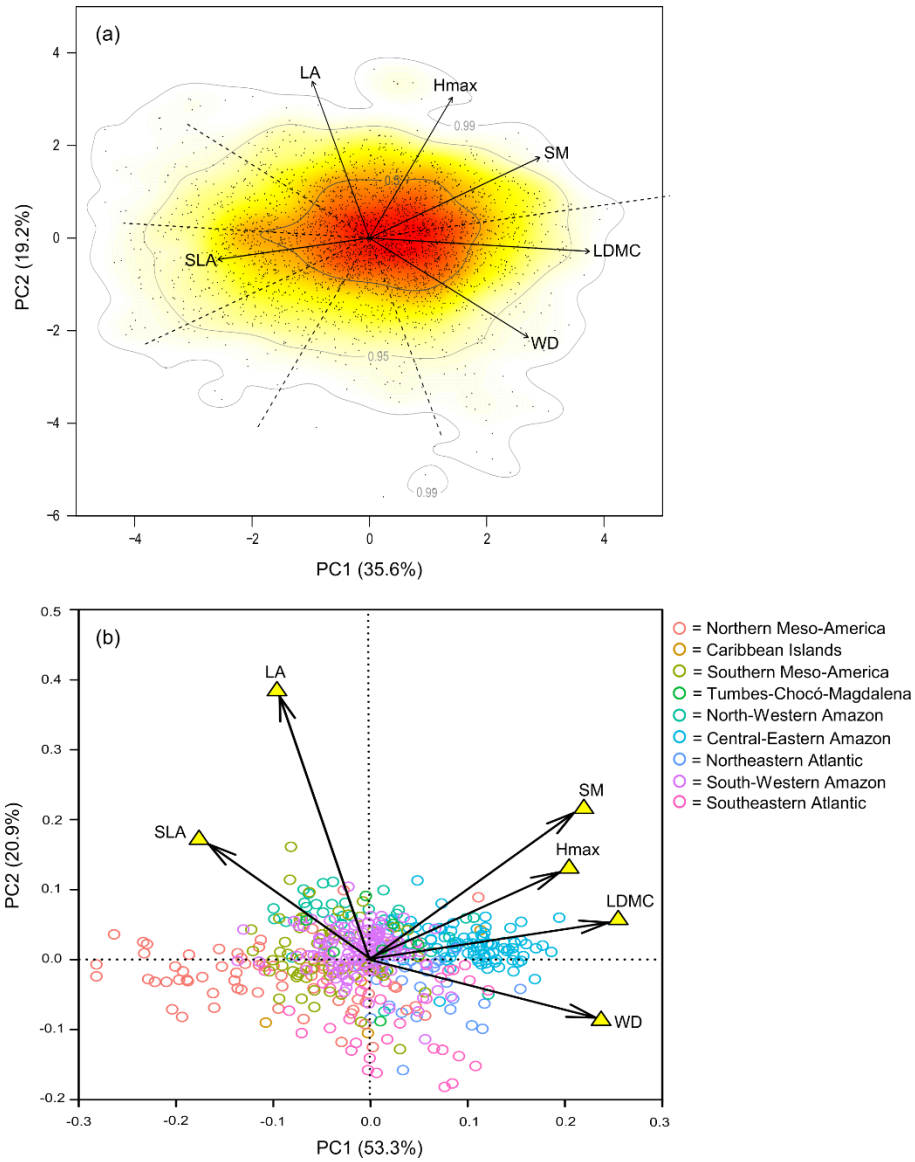


822

823 **Figure 3.** Ordination diagram of the first two axes of principal component analysis (PCA) of (a)
824 Neotropical tree species trait values (n = 3,417 species); and (b) community-weighted mean trait
825 values of tree communities (n = 471 plots) distributed across nine Neotropical moist forest re-
826 gions. The occurrence probability of species in the trait space is illustrated in (a) by color gradi-
827 ents from highest (red) to lowest (white) kernel density, with contour lines indicating 0.5, 0.95
828 and 0.99 quantiles. LA, leaf area; SLA, specific leaf area; LDMC, leaf dry matter content; WD,
829 wood density; SM, seed mass; Hmax, maximum height.

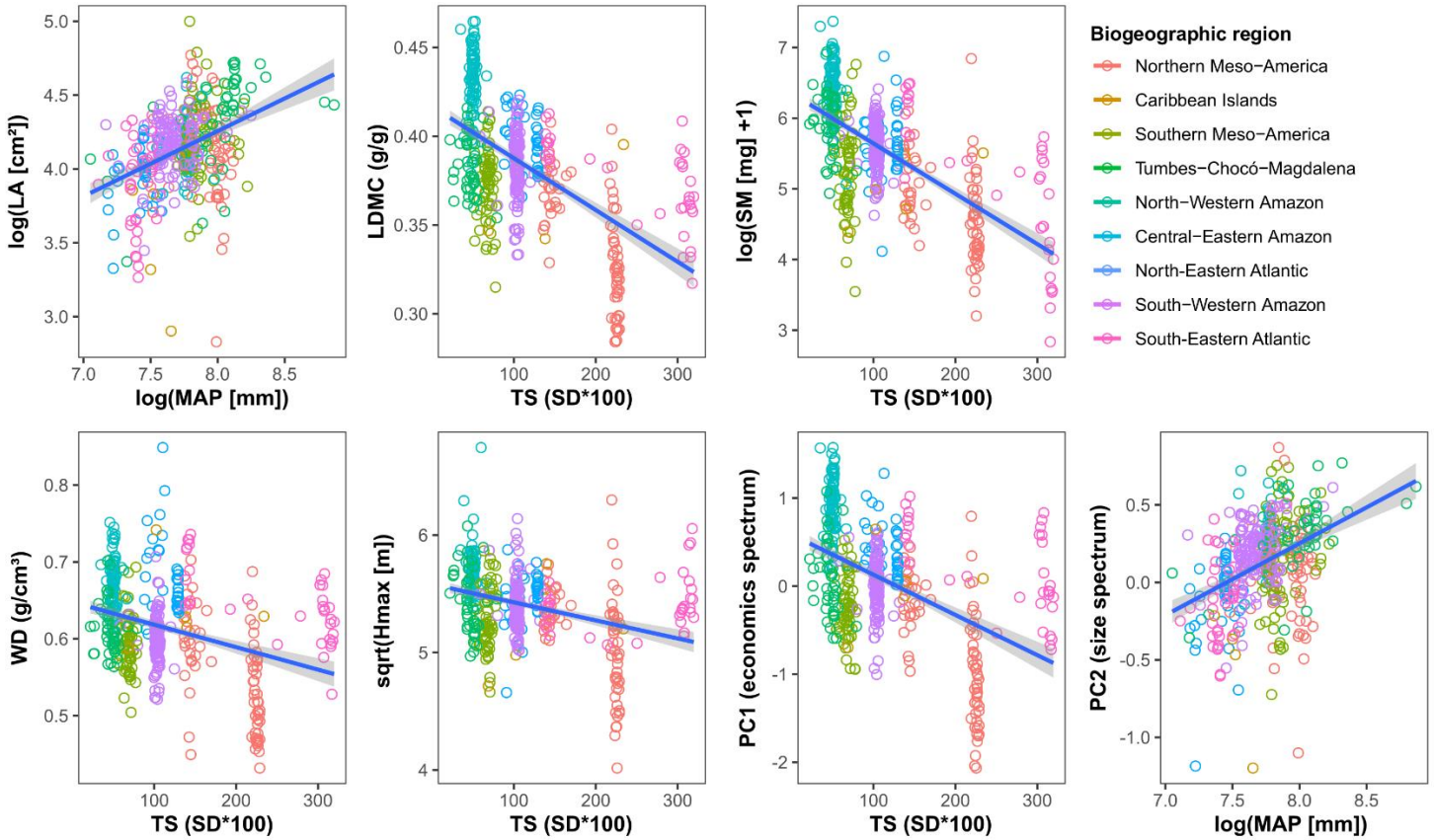


**Figure 4.** Significant relationships between climatic variables and community weighted-mean (CWM) of functional traits and strategies (i.e., species scores on the two first axes of PCA on functional traits, see Fig. 3a), for 471 tree communities distributed across nine Neotropical moist forest regions (see Table 1 for details on the best models). LA, leaf area; LDMC, leaf dry matter content; WD, wood density; SM, seed mass; Hmax, maximum height. MAP, mean annual precipitation; TS, temperature seasonality; SD, standard deviation. The relationship with highest slope (i.e., estimate) is shown for each trait/strategy, except for LA and PC2, for which we selected the relationship with the lowest error and p-value from two relationships with similar slopes.

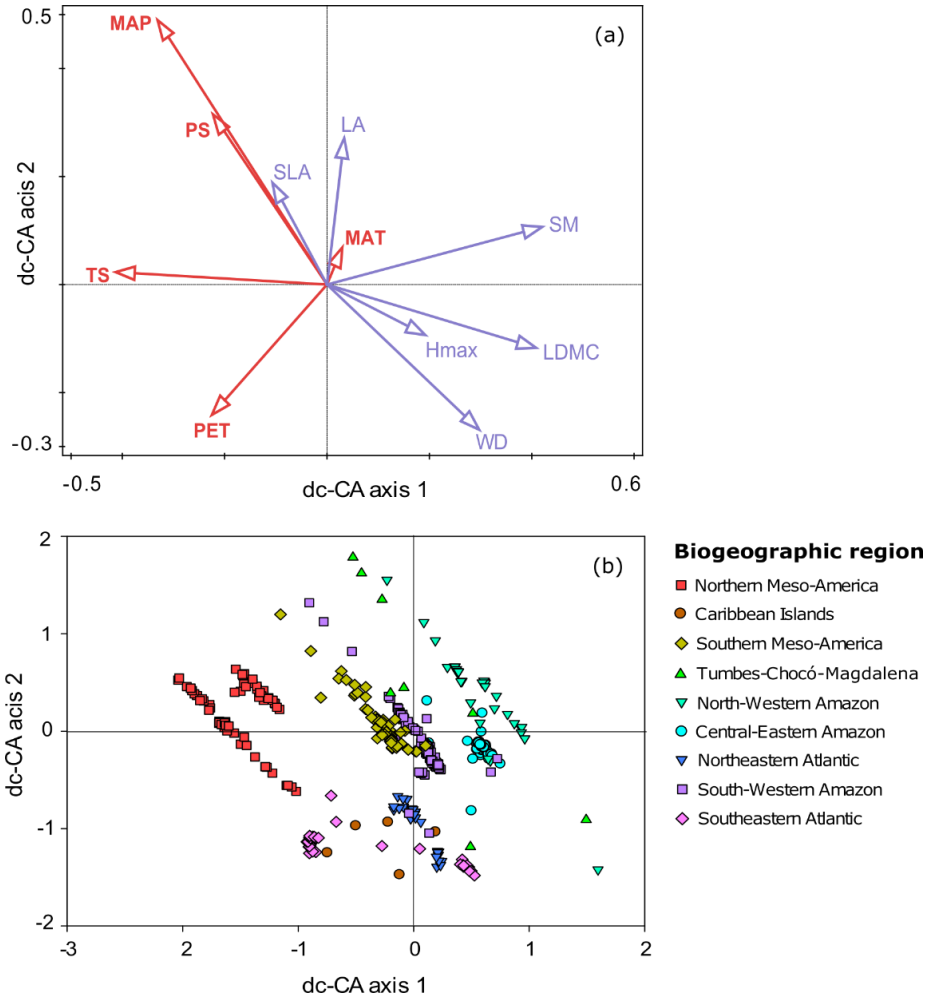


**Figure 5.** Ordination diagrams from double-constrained correspondence analysis (dc-CA) for 3,417 species across 471 Neotropical moist forest plots, showing (a) biplot of canonical weights of climate variables and scaled correlations of traits summarizing the coefficients of the multiple regressions of all CWMs of traits on the climate predictors; and (b) position (constrained scores) of samples (plots) in the dc-CA biplot. Graphs (a) and (b) form a biplot of the CWMs of all plots and traits. The significance of dc-CA results has been tested by aggregating community data by spatial clusters of plots (N = 59; see Fig. S5) to avoid pseudo-replication (see Table 2 for related statistics). The position of the 30 species which contribute most to the first two dc-CA axes is showed in Fig. S8.

**Supporting information** – Pinho et al. *Global Ecology and Biogeography*

**Table S1.** Summary of sample sizes for each Neotropical moist forest region studied.

| Region | N plots | Sampled area (ha) | N species | N trees |
|---|---|---|---|---|
| Northern Meso-America | 78 | 7.8 | 329 | 5,174 |
| Caribbean Islands | 5 | 0.50 | 96 | 412 |
| Southern Meso-America | 62 | 48.24 | 890 | 38,050 |
| Tumbes-Chocó-Magdalena | 8 | 0.8 | 259 | 542 |
| North-Western Amazon | 37 | 27.52 | 1605 | 20,008 |
| Central-Eastern Amazon | 85 | 20.3 | 493 | 9,831 |
| Northeastern Atlantic | 38 | 3.17 | 198 | 2,775 |
| South-Western Amazon | 123 | 26.66 | 1029 | 16,378 |
| Southeastern Atlantic | 35 | 3.28 | 494 | 3,120 |
| ***Neotropics*** | 471 | 138.27 | 3,417 | 96,290 |

**Table S2.** Mean trait data coverage of total plot abundances across the study regions, represented by (a) species-level data, (b) genus average, and (c) imputation. For species-level trait data, we show in parenthesis the proportion covered by authors' data. The difference between the total proportion of species-level and of the authors' data represent the proportion covered by data compiled from global databases.

| **Trait data** | N Meso-America | Caribbean Islands | S Meso-America | Tumbes-Chocó | NW-Amazon | CE-Amazon | NE-Atlantic | SW-Amazon | SE-Atlantic |
|---|---|---|---|---|---|---|---|---|---|
| ***Species-level*** | | | | | | | | | |
| (author's data) | | | | | | | | | |
| LA | 0.94 (0.92) | 0.72 (0.61) | 0.83 (0.8) | 0.51 (0.48) | 0.73 (0.71) | 0.65 (0.55) | 0.78 (0.73) | 0.84 (0.83) | 0.74 (0.71) |
| SLA | 0.94 (0.93) | 0.55 (0.49) | 0.8 (0.74) | 0.5 (0.43) | 0.69 (0.55) | 0.66 (0.42) | 0.76 (0.72) | 0.78 (0.64) | 0.72 (0.69) |
| LDMC | 0.94 (0.93) | 0.45 (0.18) | 0.75 (0.66) | 0.29 (0.47) | 0.25 (0.41) | 0.46 (0.11) | 0.7 (0.7) | 0.4 (0.35) | 0.67 (0.68) |
| WD | 0.88 (0.83) | 0.79 (0.48) | 0.85 (0.71) | 0.52 (0.38) | 0.67 (0.51) | 0.8 (0.33) | 0.84 (0.3) | 0.78 (0.65) | 0.79 (0.62) |
| SM | 0.94 (0.93) | 0.62 (0.51) | 0.78 (0.7) | 0.46 (0.41) | 0.6 (0.56) | 0.46 (0.25) | 0.72 (0.35) | 0.75 (0.7) | 0.73 (0.62) |
| Hmax | 0.87 (0.81) | 0.51 (0.33) | 0.83 (0.68) | 0.46 (0.37) | 0.66 (0.58) | 0.66 (0.34) | 0.89 (0.33) | 0.8 (0.75) | 0.86 (0.19) |
| ***Genus average*** | | | | | | | | | |
| LA | 0.06 | 0.27 | 0.16 | 0.44 | 0.23 | 0.34 | 0.22 | 0.14 | 0.24 |
| SLA | 0.06 | 0.45 | 0.19 | 0.47 | 0.28 | 0.33 | 0.24 | 0.20 | 0.26 |
| LDMC | 0.05 | 0.42 | 0.23 | 0.64 | 0.66 | 0.50 | 0.27 | 0.55 | 0.29 |

| | | | | | | | | | |
|---|---|---|---|---|---|---|---|---|---|
| WD | 0.12 | 0.19 | 0.15 | 0.44 | 0.30 | 0.19 | 0.16 | 0.21 | 0.20 |
| SM | 0.06 | 0.32 | 0.20 | 0.48 | 0.34 | 0.53 | 0.28 | 0.23 | 0.24 |
| Hmax | 0.12 | 0.47 | 0.17 | 0.49 | 0.30 | 0.32 | 0.10 | 0.18 | 0.12 |
| ***Imputation*** | | | | | | | | | |
| LA | 0.00 | 0.01 | 0.01 | 0.05 | 0.04 | 0.01 | 0.00 | 0.02 | 0.02 |
| SLA | 0.00 | 0.00 | 0.01 | 0.03 | 0.03 | 0.01 | 0.00 | 0.02 | 0.02 |
| LDMC | 0.01 | 0.13 | 0.02 | 0.07 | 0.09 | 0.04 | 0.03 | 0.05 | 0.04 |
| WD | 0.00 | 0.02 | 0.00 | 0.04 | 0.03 | 0.01 | 0.00 | 0.01 | 0.01 |
| SM | 0.00 | 0.06 | 0.02 | 0.06 | 0.06 | 0.01 | 0.00 | 0.02 | 0.03 |
| Hmax | 0.01 | 0.02 | 0.00 | 0.05 | 0.04 | 0.02 | 0.01 | 0.02 | 0.02 |

**Table S3**. Correlation between species and genus mean in the trait database studied, considering genus with at least two species with available trait data (N). All correlations were significant after adjustment for multiple comparisons ($p < 0.001$).

| **Functional trait** | **Correlation (r-pearson) species-genus mean** |
|---|---|
| Leaf area (N = 1,718) | 0.74 |
| Specific leaf area (N = 1,555) | 0.61 |
| Leaf dry matter content (N = 845) | 0.84 |
| Wood density (N = 1,643) | 0.86 |
| Seed mass (N = 1,297) | 0.73 |
| Maximum height (N = 1,653) | 0.66 |

**Table S4.** Bivariate relationships (*r*-values) between climatic variables across 471 moist forest sites distributed across the Neotropics. In addition to the five variables considered in model selection (see Table 1), correlation coefficients are also shown for variables that were initially considered but then excluded due to high variance inflation factor values or insignificant results. Strong correlations ($r > 0.7$) are highlighted in bold. MAP, mean annual precipitation (mm); MAT, mean annual temperature (ºC); PET, potential evapotranspiration (mm); PS, precipitation seasonality (coefficient of variation of monthly precipitation values); TS, temperature seasonality (standard deviation of monthly temperature values); PreDryQua, precipitation in the driest quarter (mm); SPEI, standardized precipitation-evapotranspiration index (mm); CWD, cumulative water deficit (mm).

| | MAT | PET | PS | TS | Pre-DryQua | Aridity | SPEI | CWD |
|---|---|---|---|---|---|---|---|---|
| MAP | 0.43 | 0.15 | -0.15 | -0.32 | 0.52 | **0.82** | -0.21 | 0.33 |
| MAT | | 0.31 | 0.14 | -0.67 | 0.06 | 0.19 | 0.14 | -0.08 |
| PET | | | 0.62 | 0.12 | -0.51 | -0.37 | -0.28 | -0.66 |
| PS | | | | 0.18 | **-0.84** | -0.5 | -0.03 | **-0.77** |
| TS | | | | | -0.28 | -0.35 | -0.37 | -0.07 |
| PreDryQua | | | | | | **0.83** | -0.09 | **0.74** |
| Aridity | | | | | | | -0.12 | 0.58 |
| SPEI | | | | | | | | 0.16 |

**Table S5.** Trait loadings of principal component analysis (PCA) on Neotropical tree species mean traits (n = 3,417) and community-weighted mean traits (n = 471). Traits were standardized to Z units (mean = 0, SD = 1) after being transformed. The axis with highest loading for each trait is highlighted in bold.

| Functional trait | Species-level | | | Community-level | | |
|---|---|---|---|---|---|---|
| | PC1 (35.6%) | PC2 (19.1%) | PC3 (15.0%) | PC1 (53.3%) | PC2 (20.9%) | PC3 (10.8%) |
| Leaf area | -0.193 | **0.672** | 0.513 | -0.191 | **0.765** | -0.301 |
| Specific leaf area | -0.391 | -0.070 | **-0.643** | -0.350 | 0.347 | **0.771** |
| Leaf dry matter content | **0.564** | -0.043 | 0.009 | **0.510** | 0.113 | 0.136 |
| Wood density | **0.449** | -0.356 | 0.108 | **0.475** | -0.174 | 0.374 |
| Seed mass | **0.466** | 0.279 | -0.125 | **0.433** | 0.428 | 0.226 |
| Maximum height | 0.270 | **0.580** | -0.544 | **0.409** | 0.261 | -0.325 |

**Table S6.** Statistics from double constrained correspondence analysis (dc-CA) of species abundance matrix from 59 aggregated samples (clusters of 471 forest plots, connected by maximum 50-km, see Fig. S5). Samples have been aggregated to spatial cluster means to avoid pseudo-replication. E = environmental (climate) variables; T = functional traits; CWM = community weighted mean traits; SNC = species niche centroids. Max-test consider the highest p-value across species- and community-level tests.

| Statistic | Axis 1 | Axis 2 | Axis 3 |
|---|---|---|---|
| dc-CA eigenvalues | 0.10 | 0.04 | 0.02 |
| fourth-corner correlations (rFC) | 0.31 | 0.20 | 0.12 |
| % Explained fitted variation (cum.) | 61 | 87 | 97 |
| % CWM variation expl. by E (adj R2) | 30 | 46 | 53 |
| % SNC variation expl. by T (adj R2) | 3 | 4 | 4 |
| Max test (p-value) | 0.001 | 0.004 | 0.152 |

**Table S7**. Relative effects of geographical and climate variables (the three most important according to forward selection) in driving taxonomic (CCA) and functional (dc-CA) structure on the species abundance table by aggregated samples (i.e., plots connected by maximum 50-km, see Fig. S5). The ratio represents the fraction of the trait-structured environmental variation in relation to the environment-structured variation.

| | **Explained inertia of count (species) table** | | |
|---|---|---|---|
| Species | unconstrained | Trait-constrained | **Ratio (dc-CA:CCA)** |
| Source | **CCA** | **dc-CA** | |
| ***Geography*** | | | |
| Latitude | 0.8 | 0.03 | 0.04 |
| Longitude | 0.74 | 0.06 | 0.08 |
| Degrees from equator | 0.67 | 0.07 | 0.10 |
| ***Climate*** | | | |
| Temperature seasonality | 0.71 | 0.05 | 0.07 |
| Potential evapotranspiration | 0.77 | 0.05 | 0.06 |
| Mean annual precipitation | 0.54 | 0.03 | 0.06 |

**Table S8.** Names of tree species associated with the eight-letters codes showed in Figure S7.

| Code | Species |
|---|---|
| CrotSchi | Croton schiedeanus |
| TabeDonn | Tabernaemontana donnell-smithii |
| PseuGlab | Pseudolmedia glabrata |
| RollMuco | Rollinia mucosa |
| MabeOcci | Mabea occidentalis |
| PeraGlab | Pera glabrata |
| VochGuat | Vochysia guatemalensis |
| OrthObla | Orthion oblanceolatum |
| CymbBail | Cymbopetalum baillonii |
| HyerAlch | Hyeronima alchorneoides |
| ProtHebe | Protium hebetatum |
| EschOvat | Eschweilera ovata |
| SipaAndi | Siparuna andina |
| GuapOppo | Guapira opposita |
| MatiMala | Matisia malacocalyx |
| HampNutr | Hampea nutricia |
| SapiLate | Sapium lateriflorum |
| MicrElat | Micrandra elata |
| EschCori | Eschweilera coriacea |
| DendArbo | Dendropanax arboreus |
| CecrObtu | Cecropia obtusifolia |

| | |
|---|---|
| MicoCabu | Miconia cabucu |
| LunaMexi | Lunania mexicana |
| GuarGlab | Guarea glabra |
| PogoScho | Pogonophora schomburgkiana |
| PipeSanc | Piper sanctum |
| BursSima | Bursera simaruba |
| EschTrun | Eschweilera truncata |
| HirtHebe | Hirtella hebeclada |
| AspiAust | Aspidosperma australe |

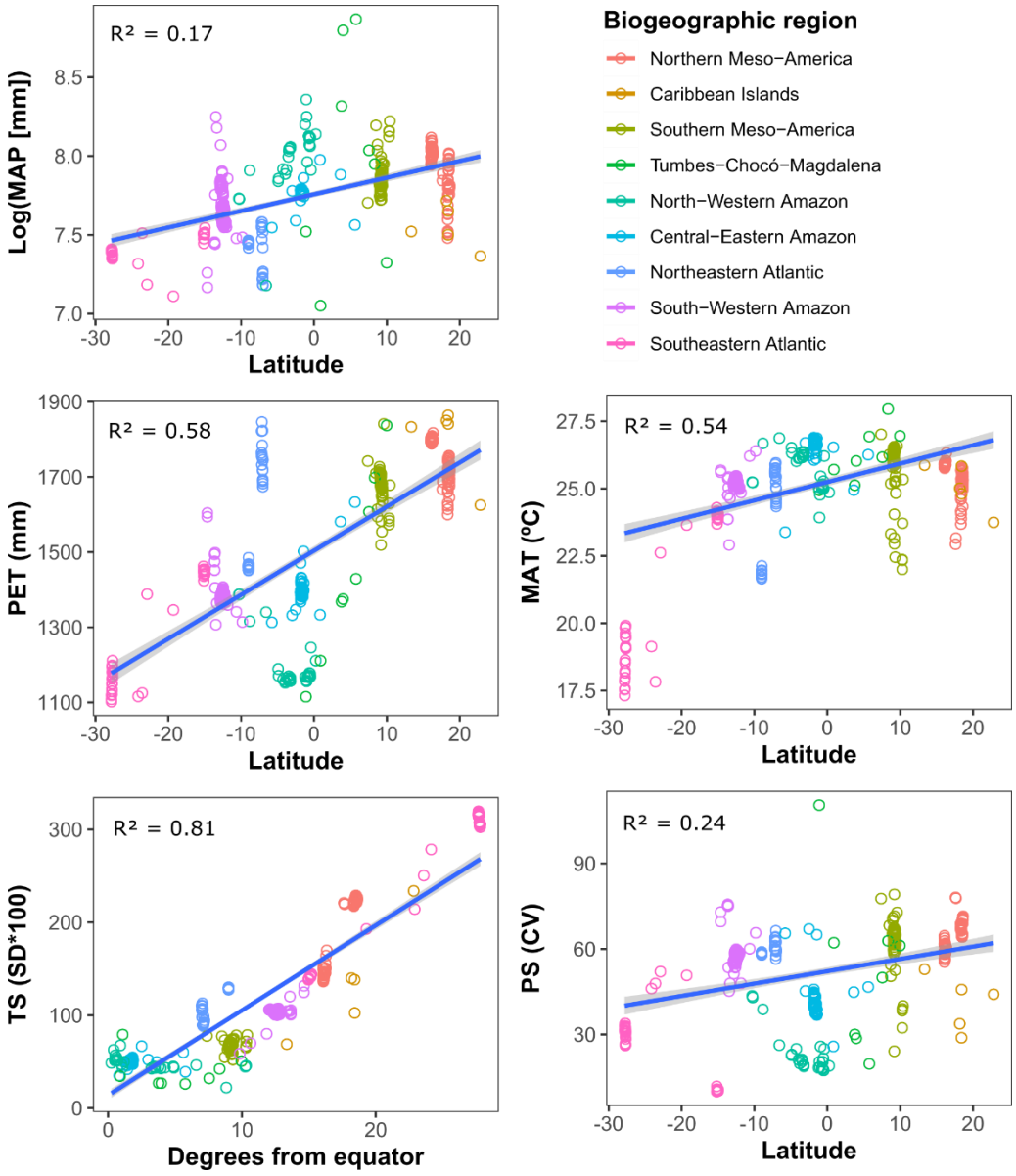


**Figure S1.** Relationships between climatic variables and latitude across 471 Neotropical moist forest plots (see Fig. 1). The variance explained is the marginal R-square from mixed-effects models with 'biogeographic region' as random factor. MAP, mean annual precipitation; MAT, mean annual temperature; PET, potential evapotranspiration; PS, precipitation seasonality; TS, temperature seasonality; SD, standard deviation of average monthly values; CV, coefficient of variation of average monthly values.

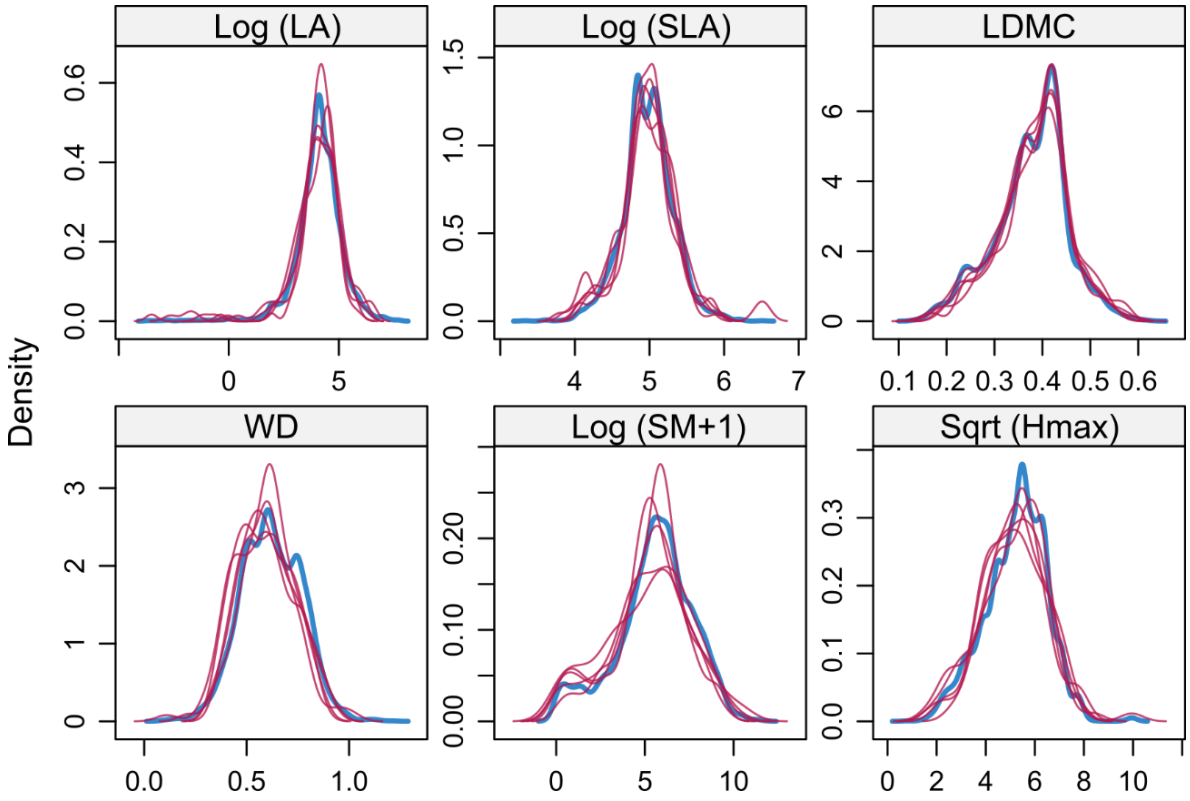


**Figure S2.** Distribution of species trait values for the original data (blue line) and five imputed datasets (red). Trait imputation was performed through chained equations by predictive mean matching, using R package 'mice'. LA, leaf area ($cm^2$); SLA, specific leaf area ($cm^2/g$); LDMC, leaf dry matter content (g/g); WD, wood density ($g/cm^3$); SM, seed mass (mg); Hmax, maximum height (m).

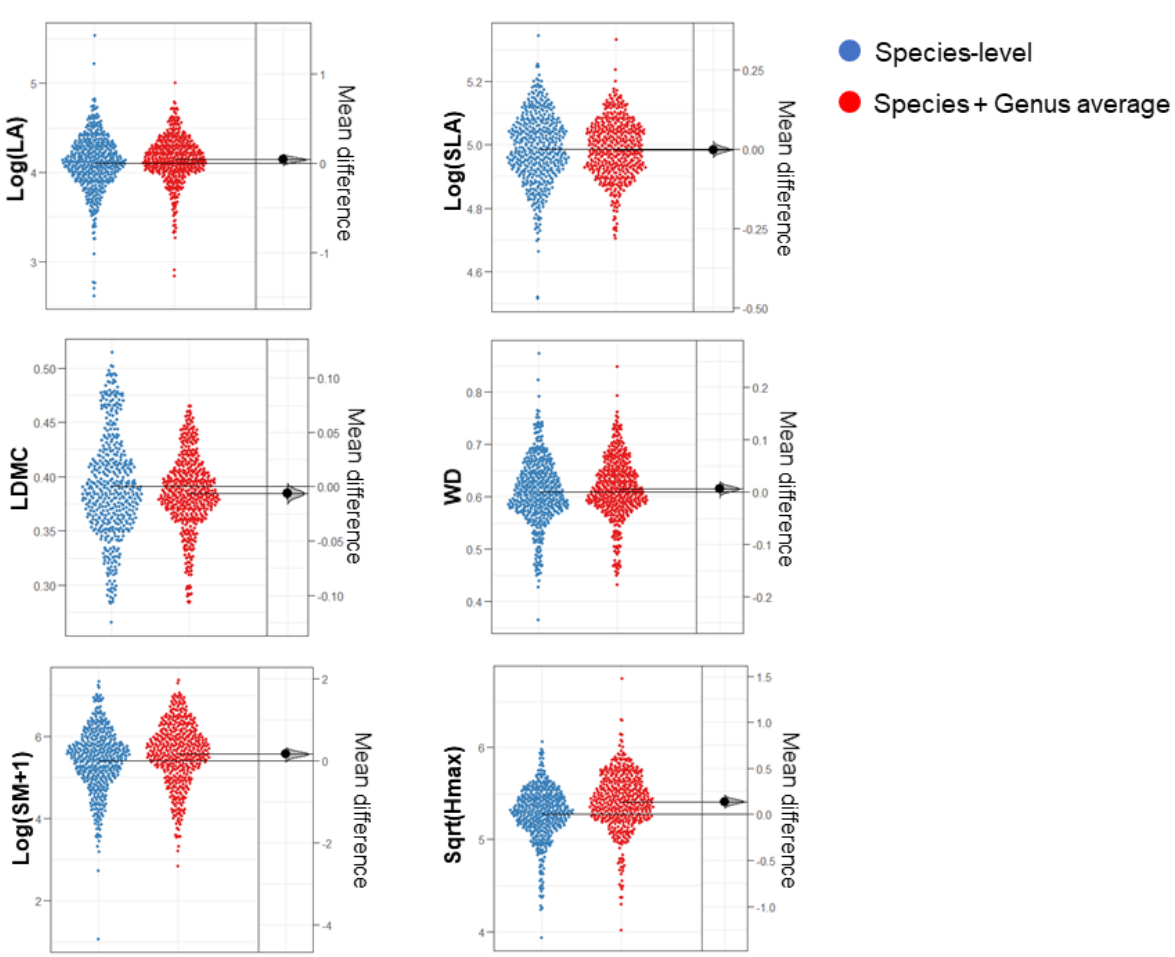


**Figure S3.** Distribution and mean differences ($p > 0.05$ according to paired-tests) of CWM trait values calculated from species-level data only (blue) and considering genus trait averages (red). LA, leaf area ($cm^2$); SLA, specific leaf area ($cm^2/g$); LDMC, leaf dry matter content (g/g); WD, wood density ($g/cm^3$); SM, seed mass (mg); Hmax, maximum height (m).

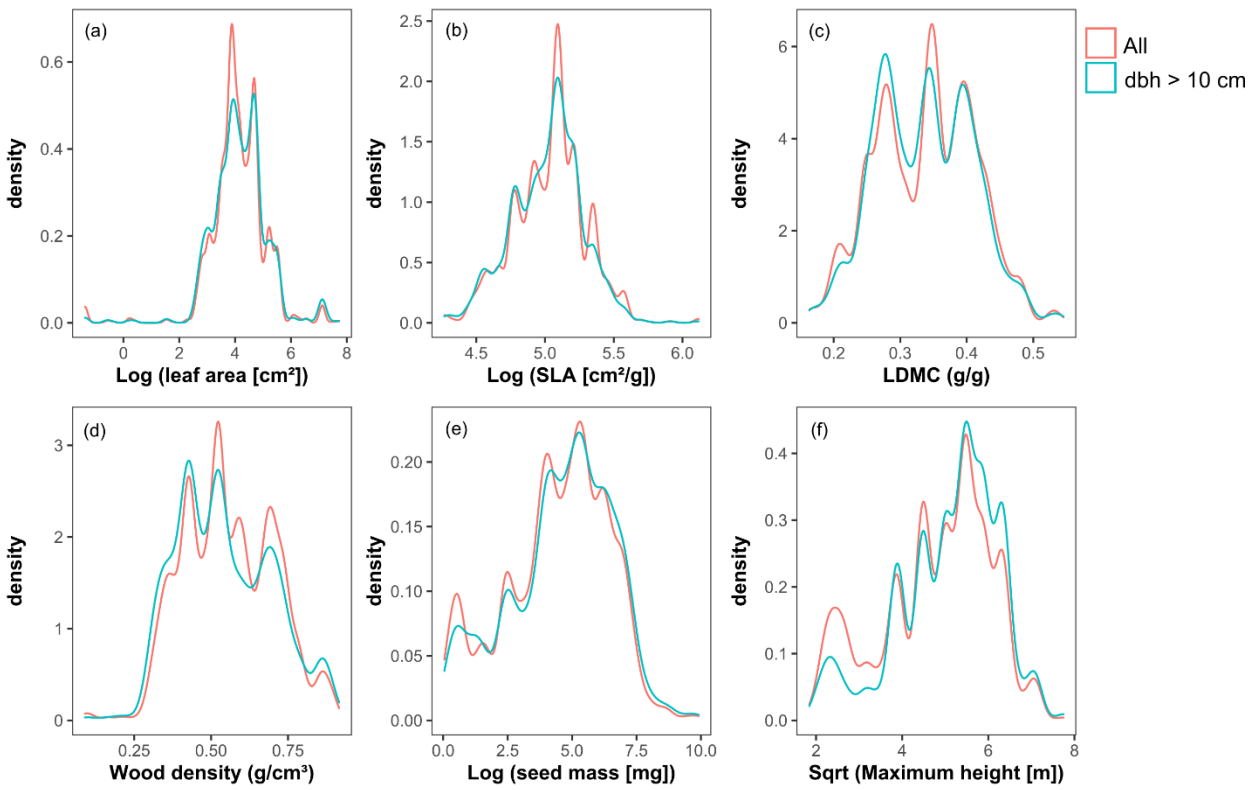


72

73 **Figure S4**. Abundance-weighted distributions of tree species trait values for all individuals with

74 diameter at breast height (DBH) from 2.5 cm (red), and for only adults with DBH > 10 cm

75 (blue), at the Northern Meso-America region.

76

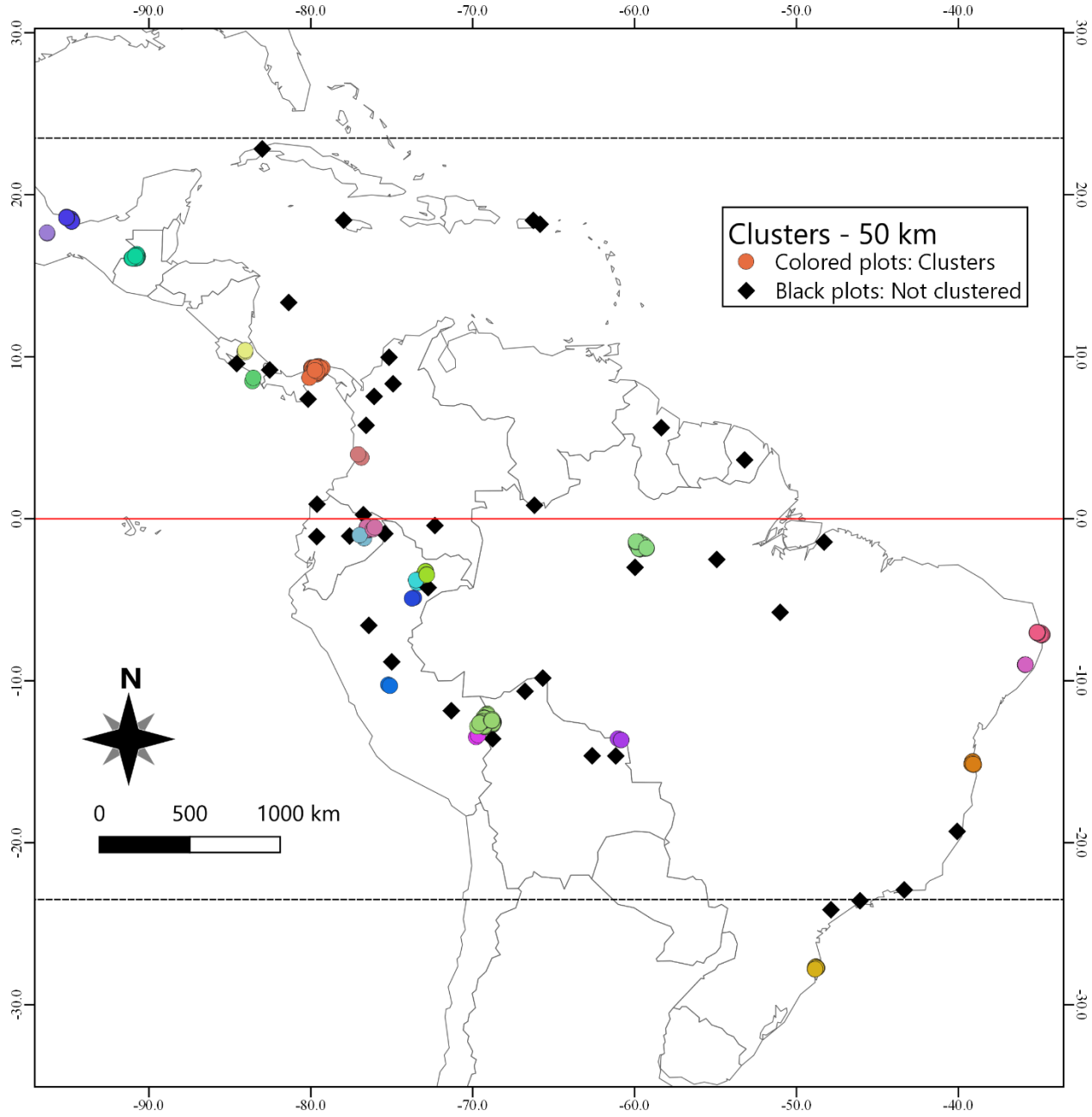


**Figure S5.** Spatial clusters (plots connected by maximum 50-km distance) that represented aggregated samples (N = 59) in double constrained correspondence analysis (dc-CA).

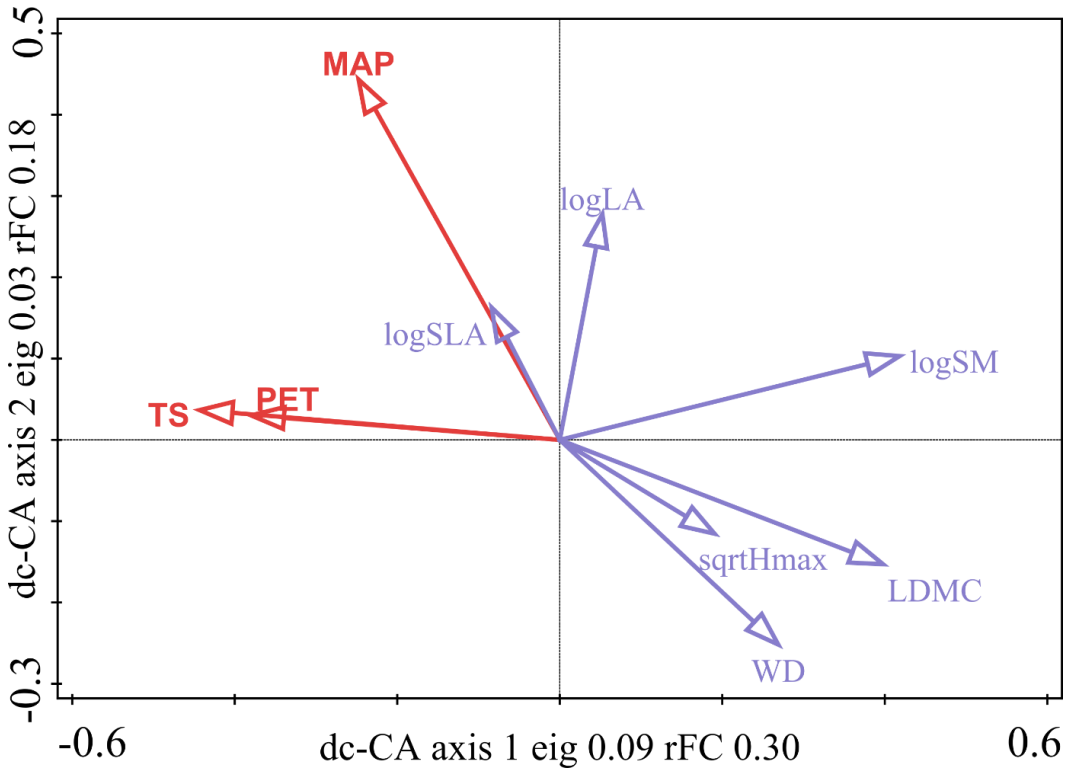


**Figure S6.** Biplot of the coefficients of the regressions of CWMs of functional traits on to the climate variables (similar to Fig. 5a), with only the three most relevant climate variables, according to forward selection in dc-CA analysis. 'eig' = eigenvalue; 'rFC' = fourth-corner correlation. MAP, mean annual precipitation (mm); PET, potential evapotranspiration (mm); TS, temperature seasonality (standard deviation of monthly values); LA, leaf area ($cm^2$); SLA, specific leaf area ($cm^2/g$); LDMC, leaf dry matter content (g/g); WD, wood density ($g/cm^3$); SM, seed mass (mg); Hmax, maximum height.

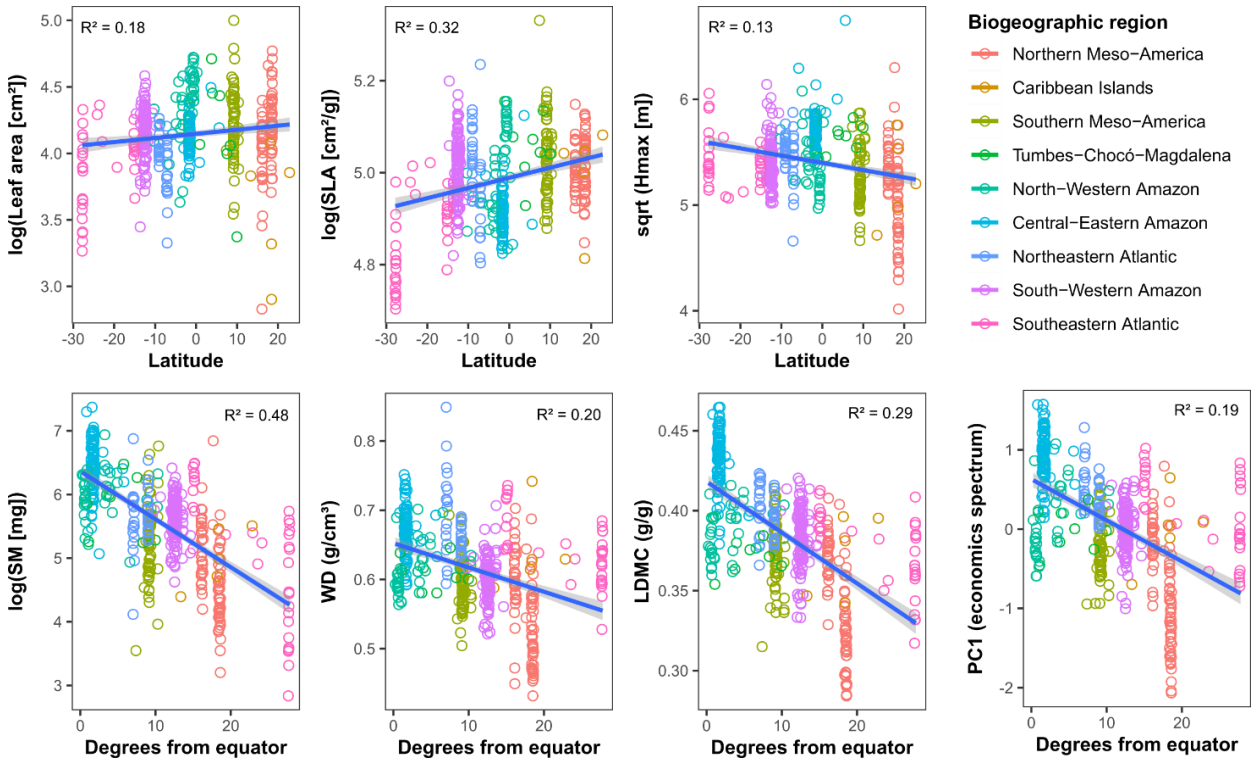


**Figure S7.** Significant relationships from mixed-effects models with latitude (south-north gradient) and degrees from equator (the strongest for each trait/strategy) as predictor of abundance-weighted community mean (CWM) of functional traits and strategies, for 471 tree communities distributed across nine Neotropical moist forest regions. The variance explained is the marginal R-square from mixed-effects models with 'biogeographic region' as random factor. LA, leaf area; SLA, specific leaf area; LDMC, leaf dry matter content; WD, wood density; SM, seed mass; Hmax, maximum height.

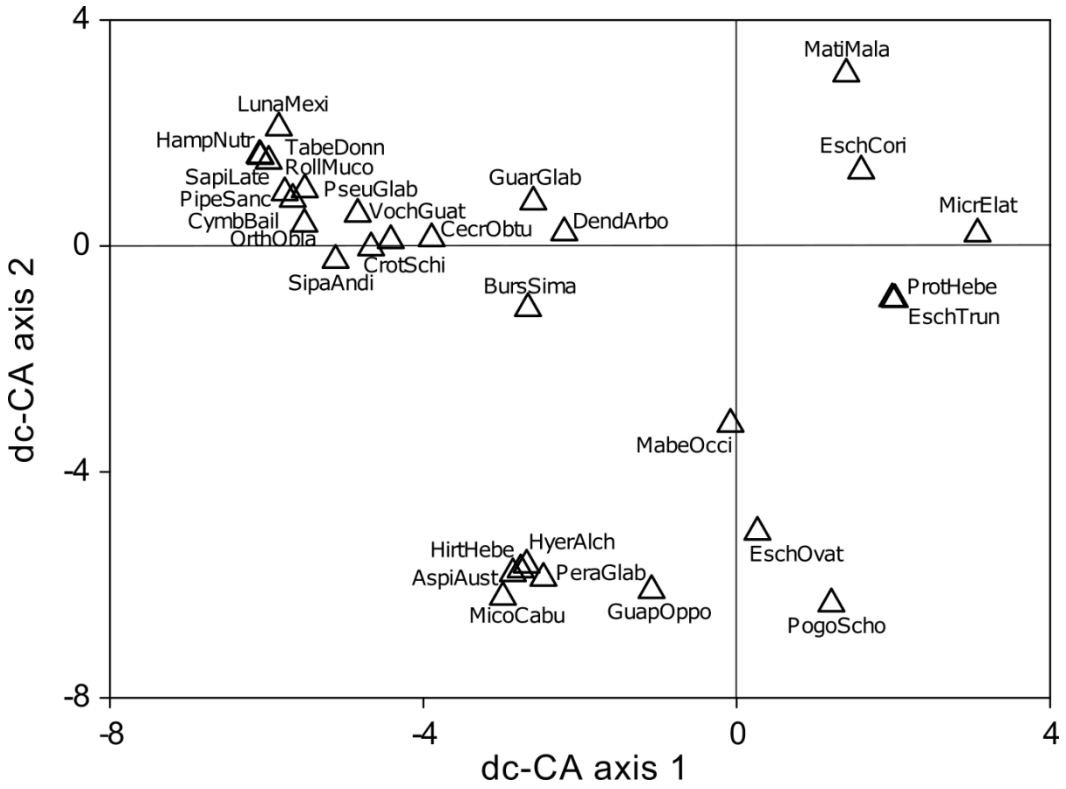


**Figure S8**. Position (unconstrained scores) on the dc-CA biplot (Fig. 5) of the 30 species which contribute most to the first two dc-CA axes. The species names associated with the eight-letter codes in are shown in Table S8.